THE EFFECT OF BIOCHAR IN ASPHALT MIXTURES

by

Oluwasewa Olanike Owolabi

B.Sc. (Civil Engineering), University of New Brunswick, 2019

A thesis Submitted in Partial Fulfillment
of the Requirements for the Degree of

Master of Science in Engineering

in the Graduate Academic Unit of Civil Engineering

Supervisor: Xiomara Sanchez, PhD., P.Eng., Civil Engineering

Examining Board: Eric Hildebrand, PhD., P.Eng., Civil Engineering
Sina Varamini, PhD., P.Eng., Civil Engineering
Gobinda Saha, PhD., P.Eng., Mechanical Engineering

This thesis is accepted by the
Dean of Graduate Studies

THE UNIVERSITY OF NEW BRUNSWICK

September 2021

©Oluwasewa Olanike Owolabi, 2021

ABSTRACT

This study investigates the effect of biochar in asphalt mixtures. Biochar was added as a filler to the asphalt mixture at 5% and 10% by weight of asphalt binder, and two sources of biochar obtained from two different pyrolysis processes were used in the study. The purpose of the study was to investigate if the addition of biochar would be beneficial in improving the rutting resistance and fracture resistance of the asphalt mixture. Previous studies investigated the effect of biochar on the asphalt binder, but the effect on the asphalt mixture has not been thoroughly investigated, hence the need for this study. From the research, it was discovered that the addition of biochar has the potential of improving the workability of the mix. Also, biochar used as a filler in asphalt could improve the cracking resistance of the mix while causing a detrimental effect on the rutting resistance and the ageing susceptibility of the mix.

DEDICATION

This thesis is dedicated to God Almighty for His grace and infinite mercies, and the author's parents, Mr. and Mrs. Owolabi for their unwavering love and support.

ACKNOWLEDGEMENTS

Special thanks to Dr. Xiomara Sanchez for introducing me to this research and being there all the way to mentor, support and educate me through the process. Without her guidance, the research process would have been endlessly frustrating.

I would like to thank the Estebauer Foundation and the Department of Civil Engineering for funding this study. My gratitude goes to CanmetENERGY Natural Resources in Ottawa, Ontario, for supplying the biochar used for the study.

I would also like to thank the laboratory technicians at the University of New Brunswick for being helpful and supportive during the experimental process. My appreciation also goes to the engineering students that assisted me in the laboratory. I would also like to thank my fellow graduate students and my family members who motivated me through the course of the project. Finally, I say thank you to God who saw me through all the highs and lows I encountered this past year.

TABLE OF CONTENTS

ABSTRACT ii
DEDICATION iii
ACKNOWLEDGEMENTS iv
TABLE OF CONTENTS v
LIST OF TABLES viii
LIST OF FIGURES ix
LIST OF SYMBOLS, NOMENCLATURE OR ABBREVIATIONS x
1. INTRODUCTION 1
1.1. Background Information 1
1.2. Problem Statement 2
1.3. Research Questions and Hypotheses 3
1.3.1. Research Question 3
1.3.2. Research Hypotheses 3
1.4. Research Goal and Objectives 3
1.4.1. Research Goal 3
1.4.2. Research Objectives 3
1.5. Research Scope 4
1.6. Assumptions 4
1.7. Thesis Layout 5
2. LITERATURE REVIEW 6
2.1. Asphalt Mixtures 6
2.1.1. Aggregates 6
2.1.2. Asphalt Binder 6
2.1.3. Types of Hot Mix Asphalt 9
2.1.4. Asphalt Additives and Modifiers 10
2.2. Biochar 14
2.2.1. Definition of Biochar 14
2.2.2. Pyrolysis for Biochar Production 15
2.3. Effect of Biochar in Asphalt Mixtures 18
2.3.1. Environmental Benefit of Using Biochar in Asphalt Mixtures 18
2.3.2. Effect of Biochar on Asphalt Binder Performance 18

3. MATERIALS AND METHODS 21
3.1. Materials 21
3.1.1. Aggregates 21
3.1.2. Asphalt Binder 22
3.1.3. Biochar 22
3.2. Samples Preparation 23
3.2.1. Incorporating Biochar in the Mix 24
3.2.2. Batching and Mixing 25
3.2.3. Determining Maximum Relative Density (MRD) 28
3.2.4. Compacting the Mix 29
3.2.5. Determining the Bulk Relative Density and Air Void Content 31
3.3. Dynamic Modulus Test 32
3.4. Flow Number Test 38
3.5. Fracture Energy and Flexibility Index Test 40
4. RESULTS AND DISCUSSION 44
4.1. Effect of Biochar on the Workability of the Asphalt Mixtures 44
4.2. Effect of Biochar on the Response of Asphalt Mixtures 46
4.2.1. Dynamic Modulus After Short Term Ageing 46
4.2.2. Dynamic Modulus After Long Term Ageing 49
4.2.3. Effect of Ageing on the Mixes Response 52
4.3. Effect of Biochar on the Rutting Resistance of Asphalt Mixture 53
4.3.1. Flow Number After Short Term Ageing 54
4.3.2. Flow Number After Long Term Ageing 55
4.3.3. Effect of Ageing in Rutting Susceptibility 56
4.4. Effect of Biochar on the Fatigue Cracking Resistance of Asphalt Mixtures 57
4.4.1. Fracture Energy and Flexibility Index of Unconditioned Samples 57
4.4.2. Fracture Energy and Flexibility Index of Conditioned Samples 59
4.4.3. Effect of Moisture on the Fatigue Cracking Susceptibility of the Mix 60
5. CONCLUSION AND RECOMMENDATIONS 62
5.1. Conclusions 62
5.2. Recommendations 65
6. REFERENCES 67
Appendix A. Asphalt Mix Design & LTPPBind Data 74
Appendix B. Dynamic Modulus Test Data and Master Curves 76

Appendix C. Flow Number Test Data 93
Appendix D. Fracture Energy and Flexibility Index Test Data 95
Curriculum Vitae

LIST OF TABLES

Table 2.1: Characteristics of Different Pyrolysis Processes (Wani et al., 2021) 17
Table 3.1: Chemical Composition of the Biochar by Weight (%) 22
Table 3.2: Nomenclature for Identifying the Asphalt Mixture Types 24
Table 3.3: Aggregate Blend Card 26
Table 3.4: Number of Gyrations Used for Compacting the Mixes 31
Table 3.5: Temperature Evaluation Parameters for LTPPBind (AASHTO T378) 39
Table 3.6: Flow Number Test Parameters (AASHTO T378) 39
Table 4.1: Dynamic Modulus of the Asphalt Mixtures After Short Term Ageing 47
Table 4.2: Dynamic Modulus of the Asphalt Mixtures After Long Term Ageing 51
Table 4.3: Effect of Long Term Ageing on the Stiffness of the Mix 52
Table 4.4: Change in the Flow Number After Long Term Ageing 56
Table 4.5: Effect of Moisture on the Cracking Potential of the Mixes 61

Table B. 1: Dynamic Modulus Test Data for the Short Term Aged Control Mix 76
Table B. 2: Dynamic Modulus Test Data for the Long Term Aged Control Mix 77
Table B. 3: Dynamic Modulus (Short Term Aged 5% Slow Pyrolysis Biochar Mix) 78
Table B. 4: Dynamic Modulus (Long Term Aged 5% Slow Pyrolysis Biochar Mix) 79
Table B. 5: Dynamic Modulus (Short Term Aged 5% Fast Pyrolysis Biochar Mix) 80
Table B. 6: Dynamic Modulus (Long Term Aged 5% Fast Pyrolysis Biochar Mix) 81
Table B. 7: Dynamic Modulus (Short Term Aged 10% Slow Pyrolysis Biochar Mix) ... 82
Table B. 8: Dynamic Modulus (Long term Aged 10% Slow Pyrolysis Biochar Mix) 83
Table B. 9: Dynamic Modulus (Short Term Aged 10% Fast Pyrolysis Biochar Mix) 84
Table B. 10: Dynamic Modulus (Long Term Aged 10% Fast Pyrolysis Biochar Mix) ... 85
Table B. 11: Fitting Parameters (Master Curve of the Short Term Aged Mixes) 92
Table B. 12: Fitting Parameters (Master Curve of the Long term Aged Mixes) 92

Table C. 1: Flow Number Test Data for the Short Term Aged Samples 93
Table C. 2: Flow Number Test Data for the Long Term Aged Samples 94

Table D. 1: Flexibility Index Test Data for the Unconditioned Specimens 95
Table D. 2: Flexibility Index Test Data for the Moisture Conditioned Specimens 96

LIST OF FIGURES

Figure 2.1: Asphalt Cement or Binder (Virginia Asphalt Association, 2020)..... 7
Figure 2.2: Asphalt Roadway (Brown & Beattie Ltd., 2018). 9
Figure 2.3: Biochar 14
Figure 2.4: Biochar Sources, Production and Applications (Wani et al., 2021)..... 15
Figure 2.5: Pyrolysis Process of Biochar (Lee et al., 2019) 16
Figure 2.6: Different Reactor Configurations (Dhyani and Bhaskar, 2019)..... 17
Figure 3.1: Aggregate Gradation of the Mix Showing the NBDTI Limits..... 21
Figure 3.2: Research Methodology Flowchart..... 23
Figure 3.3: Sieving the Biochar 24
Figure 3.4: Mixing the Biochar and Asphalt Binder..... 25
Figure 3.5: Quartering the Sample..... 27
Figure 3.6: Adding the Binder to the Aggregate and Mixing..... 27
Figure 3.7: Superpave Gyratory Compactor..... 29
Figure 3.8: Small and Large Cylinders After Compaction..... 30
Figure 3.9: Coring the Large Cylinders..... 33
Figure 3.10: Grinding the Large Cylinders..... 34
Figure 3.11: Attaching the Studs and Sensor Support Jig to the Specimen..... 34
Figure 3.12: Testing Chamber Used for the Dynamic Modulus and Flow Number Test. 36
Figure 3.13: Halving and Notching the Small Cylinders..... 40
Figure 3.14: FI Test Setup 42
Figure 3.15: Samples Before and After the FI Test..... 42
Figure 4.1: Number of Gyrations Used to Compact the Small and Large Cylinders 44
Figure 4.2: Variation in the Air Void Content of the Mix..... 45
Figure 4.3: Dynamic Modulus Master Curve After Short Term Ageing..... 47
Figure 4.4: Dynamic Modulus Master Curve after Long Term Ageing 50
Figure 4.5: Flow Number of the Asphalt Mixtures After Short Term Ageing 54
Figure 4.6: Flow Number of the Asphalt Mixtures After Long Term Ageing 56
Figure 4.7: Fracture Energy and Flexibility Index Before Conditioning..... 58
Figure 4.8: Fracture Energy and Flexibility Index After Moisture Conditioning..... 59

Figure A. 1: Type D NBDTI Mix Design Provided by GEMTEC Consulting 74
Figure A. 2: High Adjusted PG Temperature Obtained from LTPPBind..... 75

Figure B. 1: Composite Master Curve (Before and After Conditioning) 86
Figure B. 2: Master Curve of Short Term Aged vs Long Term Aged Control Mix..... 87
Figure B. 3: Master Curve (Short vs Long term Aged 5% Slow Pyrolysis Biochar)..... 88
Figure B. 4: Master Curve (Short vs Long Term Aged 5% Fast Pyrolysis Biochar) 89
Figure B. 5: Master Curve (Short vs Long Term Aged 10% Slow Pyrolysis Biochar).... 90
Figure B. 6: Master Curve (Short vs Long Term Aged 10% Fast Pyrolysis Biochar) 91

LIST OF SYMBOLS, NOMENCLATURE OR ABBREVIATIONS

AASHTO – American Association of State Highway Transportation Officials

AC – Asphalt Concrete

ASTM – American Society for Testing and Materials

DTS – Dynamic Testing System

FI – Flexibility Index

FN – Flow Number

HMA – Hot Mix Asphalt

MRD – Maximum Relative Density

NMAS – Nominal Maximum Aggregate Size

PG – Performance Grade

U.S. – United States of America

VFA – Voids Filled with Asphalt

VMA – Voids in Mineral Aggregates

1. INTRODUCTION

1.1. Background Information

Every year, the government spends a huge sum of money on repairing the roads. For instance, “the province of Quebec is estimated to spend $ 5 billion dollars on road construction and maintenance” in two years (The Globe and Mail, 2019). The damage incurred on the roadways is attributed to several factors such as climate, traffic, bad construction practices, poor aggregate gradation, etc. Another factor is the asphalt mixtures used to pave the roadways, as sometimes, raw asphalt binder does not have adequate properties to make the roadways durable. Therefore, the improvement of asphalt mixtures sometimes entails the incorporation of additives or modifiers to enhance the performance of asphalt pavements.

Various types of additives are being used and discovered from time to time. With the drive for advancement in knowledge and the need for better, durable roads, several studies have been conducted over the years on the improvement of asphalt mixtures. Some of the materials that have been used over time as asphalt additives are those that have a high carbon content in them, as they are suitable for asphalt binder since it is a hydrocarbon. An example of the additive that draws the attention of this research is the use of biochar. Biochar is a carbon-rich by-product of the thermal conversion of organic feedstocks such as wood, manure or leaves through a process known as pyrolysis. Biochar is typically the residue obtained when the pyrolysis process occurs to obtain bio-oils or biofuels. The biochar produced is considered a waste product, and since it is high in carbon content, unutilized biochar can result in environmental pollution, which in turn drives global

warming. Therefore, it is important to put the biochar to good use instead of letting it go to waste.

This study aims to examine the effect of incorporating biochar in the asphalt mix. The motivation behind this study is due to the lack of extensive research on the effect of biochar in asphalt mixes. Several studies have been conducted on the effect of biochar on the asphalt binder over time; however, not much has been done to study the effect of biochar on the asphalt mix, so this study will help bridge the gap of a lack of substantial research on the asphalt mix. This study is significant because there is a constant need for improvement as well as innovation in the asphalt and road paving industry. Also, sustainability is an essential aspect of our world today; therefore, this research contributes towards creating a more sustainable environment by reducing the carbon footprint of the society.

1.2. Problem Statement

a) Unutilized biochar can pollute the environment.

- Therefore, there is a need to put the biochar to use in order to capture the carbon and prevent it from dissipating into the atmosphere. “The use of biochar-containing construction materials to capture and then lock atmospheric carbon dioxide in buildings and structures can potentially reduce greenhouse gas emissions by an additional 25%” (Gupta and Kua, 2017).

b) Sometimes, raw asphalt binder does not have adequate properties to make the roadways durable.

- Asphalt binder often requires additives or modifiers that enhance the property of the raw asphalt binder to make it perform better. Different additives or modifiers are used to achieve various purposes.

1.3. Research Questions and Hypotheses

1.3.1. Research Question

Is the addition of biochar to the asphalt mix beneficial?

1.3.2. Research Hypotheses

The hypothesis of this study is that the incorporation of biochar does not adversely affect the mix. Also, it is hypothesized that biochar would help improve the workability of the mix by decreasing the compaction effort by a minimum of 20% based on previous investigation (Sanchez et al., 2020). Lastly, the addition of biochar would help reduce the asphalt mix susceptibility to ageing.

1.4. Research Goal and Objectives

1.4.1. Research Goal

The goal of this study is to examine the consequences of incorporating biochar in the asphalt mix.

1.4.2. Research Objectives

The goal will be accomplished through the following objectives:

- To produce control mixes in the lab containing asphalt binder and aggregates and modified mixes containing asphalt, aggregates, and biochar.

- To test the effect of adding biochar to the mix on the workability of the mix by examining the compaction effort required to make the samples.
- To test both the modified and control asphalt mix for stiffness after ageing the mix, and to understand the effect of ageing on the stiffness or dynamic modulus of the mix.
- To test both the modified and unmodified mixes for complex modulus and flow number to determine the potential for permanent deformation and low-temperature damage indirectly.
- To test the modified and control mixes using the Flexibility Index Test (FIT) to determine the fracture potential of the mixes.

1.5. Research Scope

The scope of the research entails the sieving, batching, and mixing of aggregates and asphalt binder for the control mix, as well as the addition of biochar in the modified mix. Two types of biochar at two different percentages by weight of asphalt binder were tested and compared with a set of control and conditioned samples. Part of the specimens was conditioned in the oven to simulate long term ageing, and some specimens were conditioned with a freeze-thaw cycle. This study focuses on the determination of the mix workability, dynamic modulus, flow number and fracture energy. The study was conducted at the Asphalt lab of the University of New Brunswick, Fredericton campus. The sample testing was conducted in accordance with AASHTO standards.

1.6. Assumptions

The following assumptions were made during the study:

1) The biochar is evenly incorporated in the mix and there are no residues; that is, the mix is homogenous. This assumption is made because the aggregates and modified binders will be mixed at high temperatures and for a suitable period.

2) The test results are evenly distributed; that is, the results obtained from testing the samples will follow a normal distribution curve each time the test is repeated. This assumption is made to save time while testing.

3) The experimental conditions remain constant during the experimentation period.

4) The instruments used for testing has validity and measure the desired parameters.

1.7. Thesis Layout

The section describes the structure of subsequent chapters in this thesis.

Chapter 2 aims to familiarize the reader with the background on the components of asphalt mixtures, types of hot mix asphalt, asphalt additives and biochar. The chapter also covers previous studies that have been carried out to evaluate the effect of biochar in asphalt binders.

Chapter 3 covers the materials, methodology, sample preparation, test standards, and the explanation of the laboratory tests procedures carried out in the study.

Chapter 4 explains the results obtained from the experiments, and Chapter 5 provides a summary of the findings in the study as well as recommendations for further studies.

2. LITERATURE REVIEW

2.1.Asphalt Mixtures

An asphalt mixture (mix) is typically comprised of two main components: one is the aggregate and the other, the asphalt binder. In some cases, other additives or modifiers are added to the asphalt mix to enhance or modify the property of the mix, which in turn affects the performance of the mix. Asphalt mixes are predominantly used in the construction of asphalt pavements; another term often used to refer to an asphalt mix is asphalt concrete.

2.1.1. Aggregates

The aggregates used in asphalt mixes consist of gravel, rocks, sand, stones, slag, rock dust and sometimes, recycled aggregates. Aggregates majorly support the loads in asphalt pavements, and they make up to 95 percent by weight of the asphalt mixture. There are desirable properties for the aggregates to have in asphalt mixes. These include toughness, soundness, size and gradation, cleanliness, particle shape, surface texture, absorption, and striping (Asphalt Paving Association of Iowa (APAI), 2005). The Nominal Maximum Aggregate Size (NMAS) depicts the largest size of aggregate, and it is one sieve size larger than the first sieve that retains 10% or greater of the total aggregate by mass according to the Superpave system. (National Academies of Sciences, Engineering, and Medicine., 2011).

2.1.2. Asphalt Binder

An asphalt binder, as seen in Figure 2.1, is a semi-black to brown cementitious material obtained from natural asphalt deposits or produced by the distillation of crude oil that acts

as a glue, which holds aggregates together in asphalt pavements (UG-GI-Glossary | Recycled Materials Resource Center, 2020). Asphalt binder is also referred to as "bitumen," "liquid asphalt," "asphalt cement," "mineral pitch" (Asphalt Institute, 2014). Asphalt binder is a viscoelastic material that behaves as an elastic solid at low temperatures and a viscous liquid at high temperatures.

Asphalt binder is primarily used for the construction and maintenance of highways as shown in Figure 2.2. Three types of asphalt used in asphalt pavement construction are asphalt cement, emulsified asphalts, and cutback asphalts (Asphalt Institute, 2007).

Figure 2.1: Asphalt Cement or Binder (Virginia Asphalt Association, 2020)

Emulsified asphalts are a mixture of asphalt binder, water, and emulsifying agent (Asphalt Institute, 2007). Asphalt emulsions can be used for almost any type of pavement application. They can be used for preventive and corrective maintenance on both asphalt and concrete pavements, stabilizing and reclaiming bases, building structural pavements,

and recycling worn-out pavements (Asphaltmagazine.com, 2018). Cutback asphalts are liquid asphalts manufactured by mixing asphalt binder with a petroleum solvent (gasoline, kerosene, diesel oil). They are used for maintenance in the manufacture of patching materials (Asphalt Institute, 2007).

Asphalt binder is used to make hot mix asphalt (HMA), which is utilized for road construction. Asphalt makes up most of the roads we travel on. In most cases, aggregates make up around 95% of the asphalt mix (stone, sand, and reclaimed products). The remaining 5% is liquid asphalt, which is also known as a binder since it works as a glue to hold the aggregates together.

Asphalt roads can be used for a variety of reasons. Because the demands of a local road differ from those of a freeway road, different aggregate volumes are used to match the road standard for different road types. Larger aggregates and fewer fines, for example, can be used to create a stronger, less flexible pavement, whereas fines are required for a more flexible pavement. Polymers and other additives can be used to alter the properties of the asphalt binder to increase the asphalt pavement's efficiency, workability, and life cycle.

Asphalt has been used as an adhesive and a water repellent since before the Roman era. It occurs naturally in a few places across the world, including a lake on the island of Trinidad and the LaBrea "tar pits" in downtown Los Angeles.

Figure 2.2: Asphalt Roadway (Brown & Beattie Ltd., 2018).

Asphalt binder comes in a variety of grades, with softer asphalts being used in colder areas and harder asphalts being used in hotter ones. The US government sponsored a multi-million-dollar research project (Strategic Highway Research Program, SHRP) in the 1990s, which developed new standards for asphalt binders called performance grade (PG) binders (MacInnis, 2018). A PG 58-28, for example, is designed for usage in areas where the average hottest week pavement temperatures reach 58 degrees Celsius, and the lowest temperature recorded during the year is -28 degrees Celsius. Premium grades typically contain polymers or other modifiers for heavy-duty applications such as city junctions, airports, or harsh climates.

2.1.3. Types of Hot Mix Asphalt

The most widely recognized type of flexible pavement surfacing in the U.S. is hot mix asphalt (HMA). HMA is referred to by a wide range of names, such as hot mix, asphalt concrete (AC or ACP), or blacktop. HMA is recognized by its design and manufacturing

techniques and incorporates traditional dense-graded mixes, stone matrix asphalt (SMA) and different open-graded aggregate gradations. A dense-graded mix has aggregate particles that are evenly distributed from coarse to fine and is often referred to as a well-graded HMA.

2.1.4. Asphalt Additives and Modifiers

Asphalt modification has been practiced in many forms for over 150 years. Heavier traffic patterns, new refining technology, copolymer chemistry, environmental pressure to recycle waste (rubber tires, shingles), and performance graded (PG) asphalt specifications have all contributed to the widespread growth in the use of modified asphalt binders over recent years (King et al., 2018). The increase in the number of modifiers used in asphalt cement can primarily be attributed to the following factors (Roberts et al., 1996):

- Increased demand in the traffic volume, loads and tire pressure on HMA pavements requires that HMA be more resistant to rutting.
- Superpave binder specification requires the asphalt binder to meet the stiffness requirements at high as well as low pavement service temperatures.
- Environmental and economic pressure to reuse what would be considered as waste materials and industrial by-products (such as tires, roofing shingles, and ash) as additives in HMA.
- Public agencies are willing to pay a higher initial cost for pavements with longer service life and/or a reduced risk of premature failure.

In the last two decades, asphalt binder obtained from different sources and grades of crude oil allows the composition of raw asphalt to vary. The use of additives is therefore needed

to ensure consistency and quality asphalt (National Academies of Sciences, Engineering, and Medicine., 2017).

The National Centre for Asphalt Technology (NCAT) published a list of reasons for the use of asphalt modification. Depending on the asphalt source and the average climatic conditions, the main reason for modifying asphalt is to stiffen binders and mixtures at high temperature to minimize rutting and reduce the detrimental effects of load-induced moisture damage; or to soften binders at low temperatures to minimize non-load associated thermal cracking. Asphalt is also modified to improve the fatigue resistance of HMA mixtures, enhance asphalt-aggregate bonding to reduce stripping or moisture susceptibility, or boost abrasion resistance to reduce ravelling. Furthermore, modifying asphalt helps rejuvenate aged asphalt binders and minimizes tender mix problems during construction. Other reasons to modify asphalts include (Roberts et al., 1996):

- Replace asphalt cement as an extender
- Permit thicker asphalt films on aggregate for increased mix durability
- Reduce flushing or bleeding
- Improve resistance to ageing or oxidation
- Reduce the structural thickness of pavement layers
- Reduce life-cycle costs of HMA pavements
- Improve overall performance of HMA pavements.

The primary benefit of using modified asphalt is to improve rutting resistance with less thermal cracking in cold temperatures and to improve durability. Some modified binders also provide improved stripping or moisture damage resistance. Some common types of asphalt cement and HMA modifiers are fillers, extenders, rubbers (elastomers or elastics),

plastics (plastomers), rubber-plastic combinations, fiber, oxidants, antioxidants, hydrocarbon, antistripping agents, waste materials and chemical modifiers (National Academies of Sciences, Engineering, and Medicine., 2017).

Fillers, as their name implies, are used to filling voids between the coarse and fine aggregates and they reduce the optimum asphalt content. They are also used to meet aggregate gradation specifications, increase stability, and improve the asphalt-cement aggregate bond. Examples of these are mineral filler, crusher fines, limes, Portland cement, fly ash, and carbon black. In this study, biochar was used as a filler. Fillers typically modify the properties of asphalt binders and impact the volumetric properties of asphalt mixtures. Mineral fillers act as an active component in asphalt mixtures due to their surface characteristics and relatively small size (passing sieve size opening of 0.075 mm). Therefore, the effect of mineral fillers is noticeable in the asphalt binder properties (Bardini et al., 2013).

Extenders are used as a substitute for a portion of asphalt cement, normally between 20 – 35 % by weight of total asphalt binders, to reduce the amount of asphalt cement used. Examples are Sulphur and lignin (Pavement Interactive, 2018).

Fibers that are natural such as asbestos, have been used for many years; however, asbestos is no longer used in the US since identified to pose health hazards. Instead, manufactured or synthetic fibers have been used to replace asbestos. Fibers can reinforce and improve the tensile strength and cohesion of HMA mixtures. They permit higher asphalt content without any significant drain down problem (Roberts et al., 1996). Oxidants are used to increase HMA stiffness after the HMA has been placed. An example is manganese salt (Pavement Interactive, 2018).

Antioxidants are used to increase the durability of HMA mixtures by delaying their oxidation. Examples are lead compounds, carbons, and calcium salts. Hydrocarbons are used to restore aged asphalt cement to current specification and to increase HMA stiffness in general. Examples are recycling and rejuvenating oils, hard and natural asphalts. Antistripping agents are used to minimizing the stripping of asphalt cement from aggregates. Examples are amines and limes. Waste materials are used to replace aggregate, or the quantity of asphalt used to recycle and save cost. Examples are roofing shingles, recycled tires and glass (Pavement Interactive, 2018).

The most used chemical modifier is polyphosphoric acid. This modifier may be used in combination with polymers to increase the high-temperature stiffness of asphalt binders (Walker, 2018). Plastics, rubbers, and plastic-rubber combinations can be grouped under the generic term "polymers." Polymers cover a wide range of modifiers, with plastomers (plastic) and elastomers (rubbers or elastics) being the most used types. Styrene-butadiene rubber, styrene-butadiene-styrene (SBS), and crumb rubber are frequently used elastomers, with SBS being the most frequently used modifier. These modifiers are used to reduce rutting and to improve fatigue and thermal cracking resistance. Crumb rubber is an elastomer made from ground tires. This material is used primarily to address rutting and fatigue. Plastomers are used to improve the high-temperature (rutting) properties of modified materials. Low-density polyethylene (LDPE) and EVA are examples of plastomers used in asphalt modification (National Academies of Sciences, Engineering, and Medicine., 2017).

2.2.Biochar

This section explains what biochar is, its application and the production process of biochar from biomass.

2.2.1. Definition of Biochar

Biochar is a carbonaceous by-product from converting plant matters such as wood to biofuels through the process of pyrolysis (Zhao et al., 2014). Pyrolysis is the thermo-chemical conversion of dry organic materials (i.e., woody wastes) into bio-oil, syngas, and biochar. "Biochar is a carbon-rich by-product of the thermal conversion of organic feedstocks" (Avanthi et al., 2017).

Biochar is a charcoal-like substance shown in Figure 2.3. Although by merely looking at it, biochar, charcoal, and activated carbon look the same, and they have a common production process (pyrolysis). They also have a similarity in their chemical composition as they contain aromatic carbons strongly bound together to make them stable. However, these three substances are different in their application. Biochar is used in agriculture for soil remediation and carbon sequestration, charcoal is used for cooking and heating, and activated carbon is used for filtration and purification processes (McLaughlin, 2016 & CharGrow, 2018).

Figure 2.3: Biochar

2.2.2. Pyrolysis for Biochar Production

The pyrolysis process is a controlled endothermic reaction that converts biomass or organic materials from forestry and agricultural wastes in the presence of little to no oxygen at high temperatures into a stable form of carbon that can be safely stored (Spears, 2018) and used for other purposes. For example, biochar is used in agriculture for soil remediation (Koul et al., 2018, & Zama et al., 2018, & Cheng et al., 2020). Figures 2.4 and 2.5 highlight the sources of biomass, the production process of biochar, and the engineering applications of biochar.

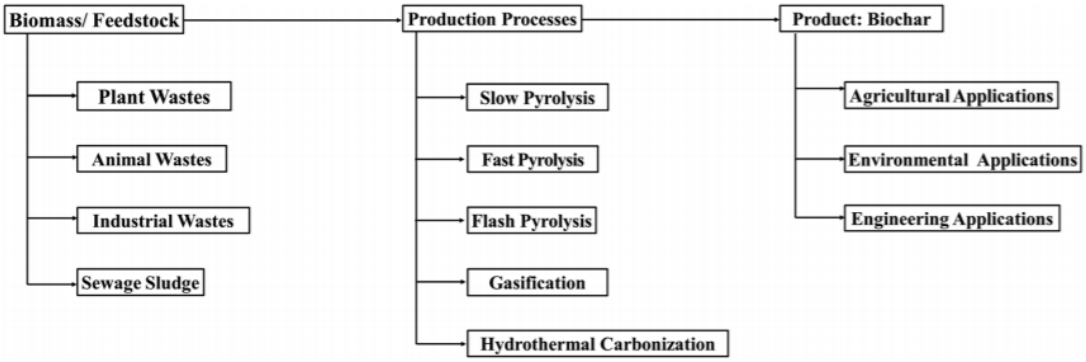

Figure 2.4: Biochar Sources, Production and Applications (Wani et al., 2021)

The yield and properties of biochar obtained during pyrolysis depend on factors such as the type of feedstock or biomass, temperature, pressure, and exposure time of the biomass to the heat source, also known as retention time (Jeguirim and Limousy, 2017 & Hersh et al., 2019). During the pyrolysis of biomass, solids, liquid, and gases are produced. The solid obtained is the biochar; the liquids are referred to as bio-oils, and the gases are often termed as syngas (Townsend, 2016). Biochar can be produced from different processes, as presented in Figures 2.4 and 2.5. Slow pyrolysis, also known as conventional carbonization, is the process of heating biomass at a low temperature and long vapor

residence time. The inverse is the case for fast pyrolysis, which is the process of heating biomass at a high temperature and short vapor residence time. The slow pyrolysis process produces a higher yield of biochar, as the yield decreases when the temperature increases. The fixed-carbon content also increases with an increase in temperature. The fast pyrolysis process produces a higher liquid (bio-oil) yield. Gasification is a thermochemical process of converting carbonaceous feedstock into a non-condensable gas at high temperatures (Manyà, 2012).

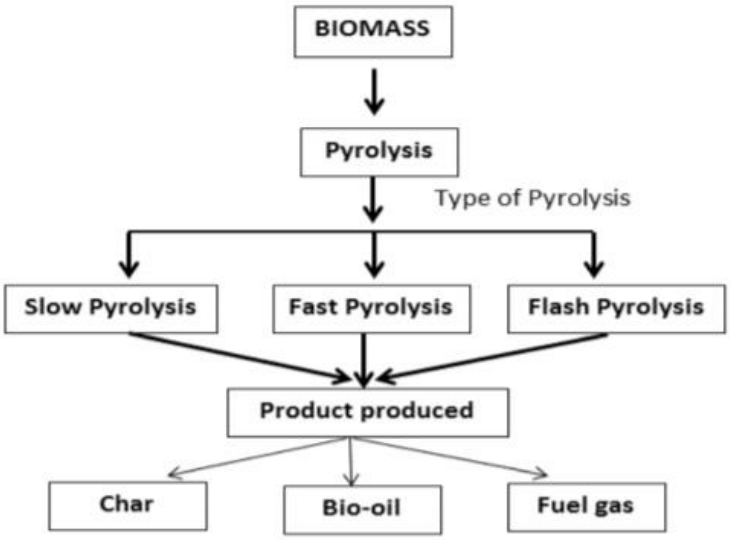

Figure 2.5: Pyrolysis Process of Biochar (Lee et al., 2019)

Flash pyrolysis, also referred to as ultra-fast pyrolysis or very fast pyrolysis, is a very rapid thermal decomposition of biomass at a high heating rate and a very short retention time (Basu, 2010). Table 2.1 summarizes the differences between the pyrolysis process. Hydrothermal carbonization (HTC) is a thermochemical process of converting wet biomass feedstock to hydrochar. The advantage of HTC is that it can process wet waste without the need for drying the feedstock beforehand (Sivaprasad et al., 2021).

Table 2.1: Characteristics of Different Pyrolysis Processes (Wani et al., 2021)

Pyrolysis Conditions	Slow	Fast	Flash	Gasification
Temperature (°C)	300 - 800	400 - 600	400 - 1000	750 - 1000
Heating rate (°C/min)	5 - 7	300 - 800	~ 1000	-
Vapor residence time	> 1 h	0.5 - 10 s	< 2 s	10 - 20 s
Biochar yield (weight %)	35 - 50	15 - 35	10 - 20	10 - 20

The process of thermally converting biomass is carried out in a specially designed chamber that captures the emissions produced. The chambers are called reactors or pyrolizers. There are different types of reactor configurations, as seen in Figure 2.6.

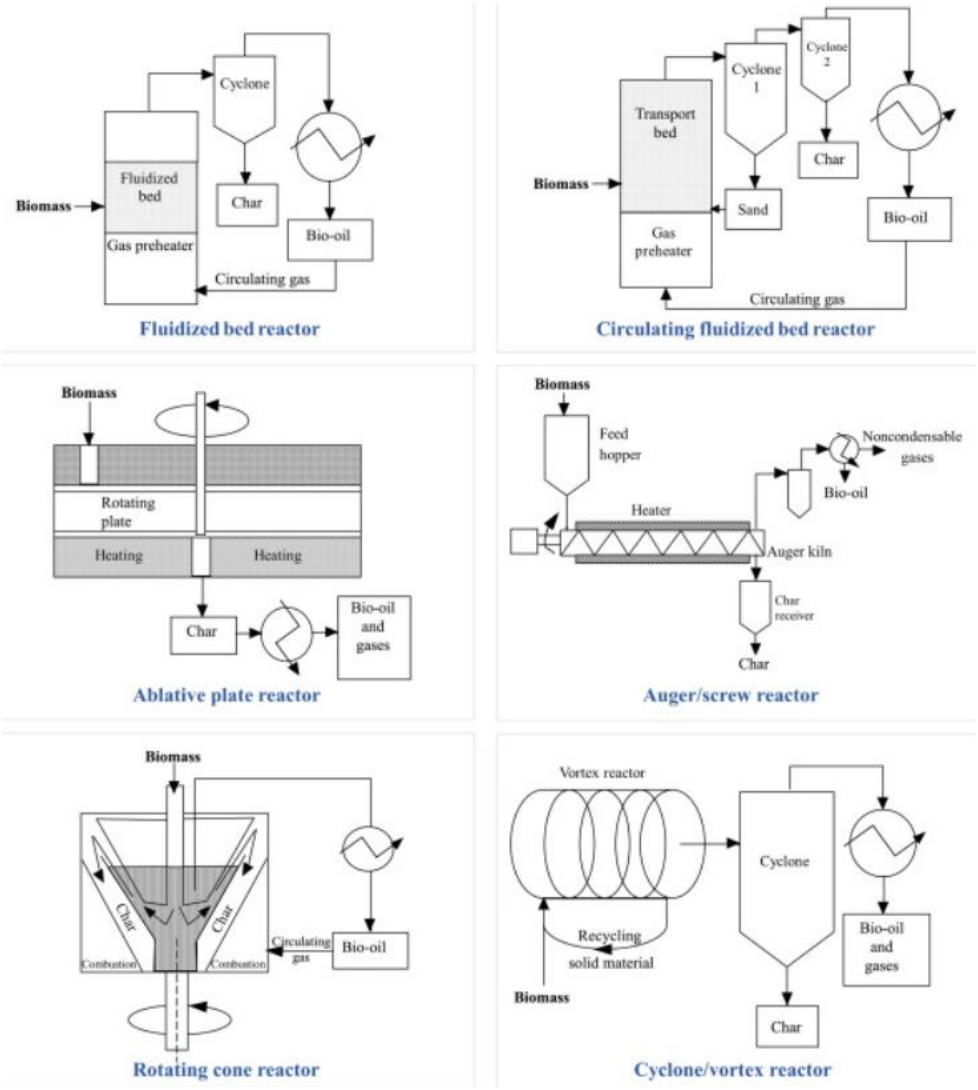

Figure 2.6: Different Reactor Configurations (Dhyani and Bhaskar, 2019)

2.3.Effect of Biochar in Asphalt Mixtures

Several studies have been conducted on the use of biochar as an asphalt modifier due to the evolving nature of the world today, which places value and emphasis on sustainability due to global warming and climate change. Biochar, which is created as a by-product of the production of bio-oils, is a highly carbonaceous substance. Instead of letting the biochar go to waste and pollute the environment, research is being done to put the biochar to use. One of the current areas of application being considered is asphalt pavements.

2.3.1. Environmental Benefit of Using Biochar in Asphalt Mixtures

The use of biochar-containing construction materials to capture and then lock atmospheric carbon dioxide in buildings and structures can potentially reduce greenhouse gas emissions by an additional 25%. Biochar's potential to be used as a carbon capturing and sequestering construction material depends on factors like the pyrolysis condition, which includes the pyrolysis temperature, heating rate, and pressure, as well as the activation methods without surface modification (Gupta and Kua, 2017). Carbon sequestration is the process of storing carbon for a long time which prevents the emission of greenhouse gases (GHG) into the atmosphere (Tan et al., 2017). The carbon stored needs to be transformed from an active state to an inert, passive state (Campbell et al., 2018).

2.3.2. Effect of Biochar on Asphalt Binder Performance

One of the benefits of incorporating biochar in an asphalt binder is that the binder becomes less susceptible to temperature. The use of biochar in the asphalt mix helps reduce the temperature susceptibility of the binder and thus increases the rutting, moisture, and

cracking resistance of hot-mix asphalt (Zhao et al., 2014, & Renaldo et al., 2014, & Chebil et al., 2002, & Kumar et al., 2018).

In a study where asphalt binders obtained from two sources were mixed at different percentages by weight of biochar, it was deduced that biochar obtained as a by-product during pyrolysis of Mesua ferrea seed cover waste could be a suitable additive to enhance the performance of asphalt binders. Adding biochar to the asphalt mix improves the permanent deformation resistance at high-service temperatures and decreases the susceptibility towards the ageing of the binder. The study also revealed that depending on the source of the asphalt binder; there might be a difference in how significant the improvement is (Kumar et al., 2018).

Also, the addition of by-products from pyrolysis helps to improve the viscosity and elasticity of the asphalt binder (Kumar et al., 2018 & Chebil et al., 2002). Zhao et al. (2014) evaluated the feasibility of using biochar obtained from pyrolyzing switchgrass as an asphalt modifier. The method of pyrolysis, the amount of modifier added, the sizes of the modifier particles, and the highest treatment temperatures (HTT), which are factors that could affect how the modified binder would respond, were considered in the study.

From the study, it was concluded that biochar improves the rheological properties of the asphalt binder and its performance against major distresses that occur in asphalt pavements. The modified binder may be beneficial in reducing oxidation of the asphalt binder after long term ageing. Also, the incorporation of biochar does not compromise the cracking resistance of the asphalt binder. In addition, biochar is a better asphalt modifier than carbon black and carbon fiber (Zhao et al., 2014).

Zhou and Adhikari (2019) also studied the flow-induced crystallization of bio-asphalt modified with different contents of biochar under various ageing conditions. From the test conducted, they were able to determine that the addition of biochar could improve the flow-induced crystallization and enhance the high-temperature properties of bio-asphalt. Biochar is used to enhance dispersion and liquid retention while improving resistance to oxidation (Walters et al., 2015). Renaldo et al. investigated the chemical and physical properties of biochar and concluded that the presence of carbon could enhance the flow properties of asphalt binder and reduce the binder oxidation during ageing (Renaldo et al., 2014). The anti-ageing effect of biochar in asphalt binder is limited, so after a certain percentage of biochar has been introduced in the binder, it reaches a peak where it no longer yields a better result (Wenhao et al., 2020).

From the study carried out, it can be noted that a substantial amount of research has been done on evaluating the use of bio-oils and biochar in asphalt binder. However, sufficient research has not been carried out on the effect of biochar in the asphalt mix, which includes the asphalt binder or bitumen; the biochar, which acts as the binder modifier; and the aggregates. This gap in the research facilitates the need for further studies.

3. MATERIALS AND METHODS

3.1.Materials

3.1.1. Aggregates

The aggregate used for the study was obtained from Springhill quarry and was collected in the summer of 2019. The aggregates consisted of 37% gravel, 41% dirty sand, 14% washed sand, and 8% blend or Colter sand. The batching of the aggregates was adapted from the Type D asphalt mix design developed by GEMTEC Consulting Engineers and Scientists (Appendix A, Figure A. 1). The Type D asphalt mix design is typically used in New Brunswick, and the designation "D" represents a hot mixed asphalt concrete surface mix. The nominal aggregate size of the mix was 9.5 mm. Figure 3.1 shows the aggregate gradation used for the mix.

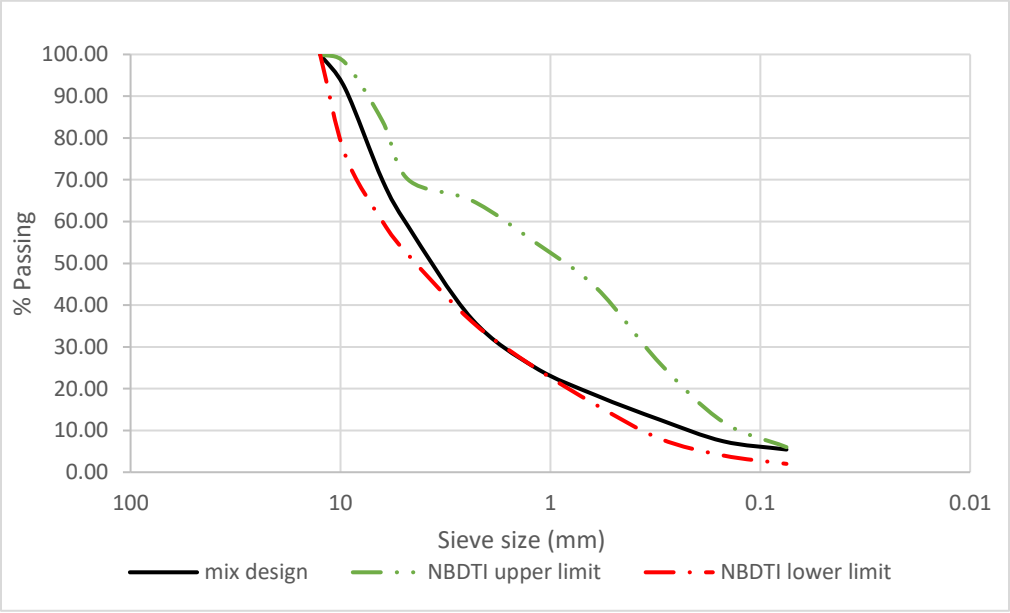

Figure 3.1: Aggregate Gradation of the Mix Showing the NBDTI Limits

3.1.2. Asphalt Binder

The asphalt binder used for the study was sourced from McAsphalt Industries Limited. The asphalt binder is a PG 58-28 binder, which is the performance grade of the asphalt binder typically used in New Brunswick. It represents an average seven-day maximum pavement temperature of 58 °C and a minimum expected pavement temperature of -28 °C. The asphalt binder used has a mixing temperature of 148 °C and a compaction temperature of 135 °C.

3.1.3. Biochar

Two types of biochar were used in this study, and they were provided by CanmetENERGY Natural Resources Canada in Ottawa, Ontario. One of the biochar was obtained from the slow pyrolysis of white birch, and the other biochar used was obtained from the fast pyrolysis of poplar bark. The biochar obtained from the fast pyrolysis of poplar bark can have a self-heating problem in the presence of air when dry, which can lead to spontaneous combustion, so water was added to the biochar to make it wet before it was supplied. The chemical composition of the fast and slow pyrolysis biochar is presented in Table 3.1.

Table 3.1: Chemical Composition of the Biochar by Weight (%)

Chemical Name	Fast Pyrolysis	Slow Pyrolysis
Ash	30.48	1.42
Volatiles	25.89	-
Fixed Carbon	39.85	-
Carbon	53	82
Hydrogen	2.79	2.85
Nitrogen	0.47	0.46
Sulphur	<0.05	<0.05
Oxygen	9.48	9.63

3.2.Samples Preparation

This section covers the processes taken to conduct the laboratory experiment, from making the mix to conditioning and testing the samples. Laboratory experiments were conducted to investigate the effect of biochar in hot mix asphalt mixtures. The laboratory experiment plan is presented in Figure 3.2.

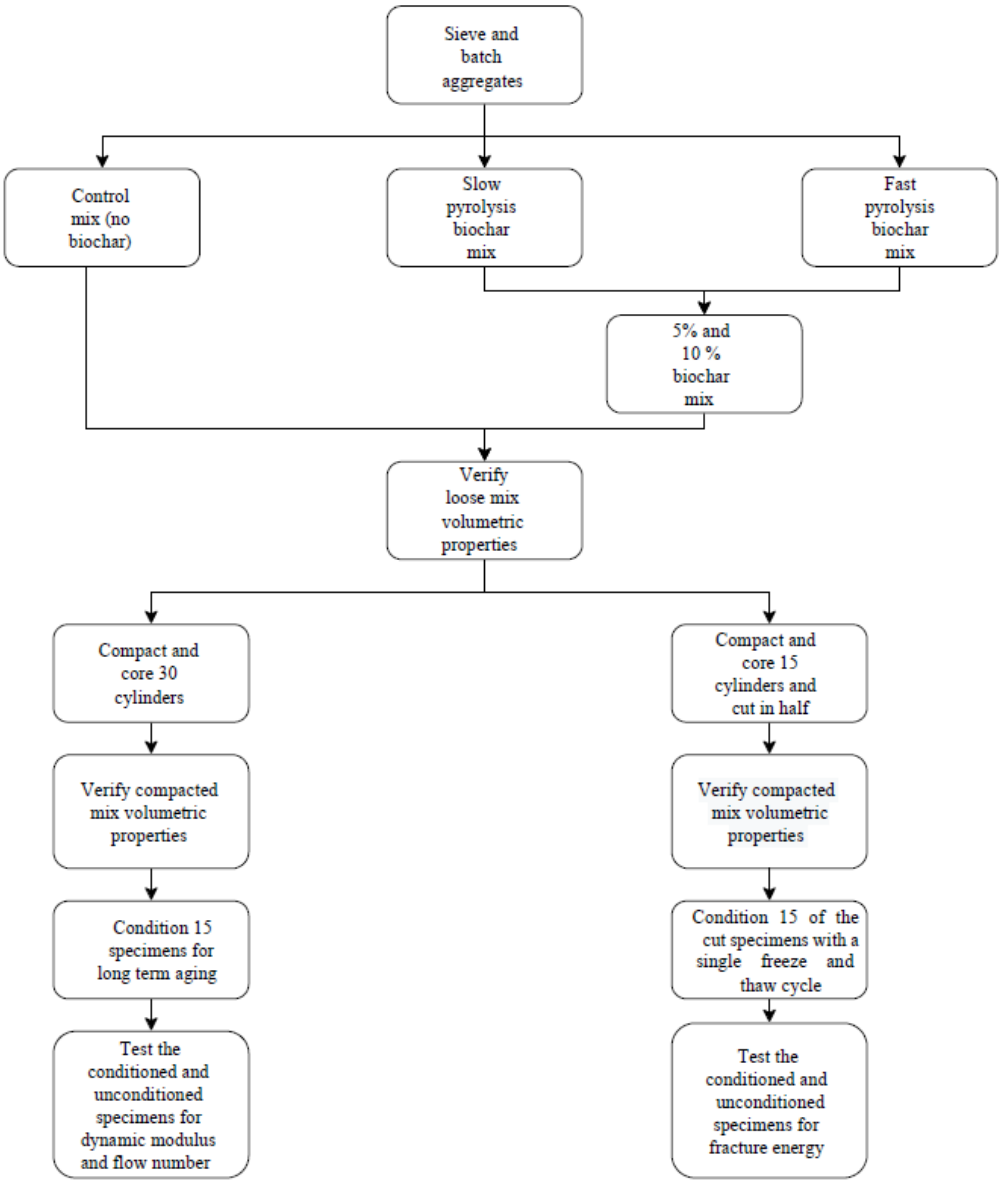

Figure 3.2: Research Methodology Flowchart

Table 3.2 represents the nomenclature used to identify the different types of mixes.

Table 3.2: Nomenclature for Identifying the Asphalt Mixture Types

Nomenclature	Type of asphalt mixture
Control	Asphalt mixture samples with 0% biochar content
BS5	Asphalt mixture samples with 5% slow pyrolysis biochar
BF5	Asphalt mixture samples with 5% fast pyrolysis biochar
BS10	Asphalt mixture samples with 10% slow pyrolysis biochar
BF10	Asphalt mixture samples with 10% fast pyrolysis biochar

3.2.1. Incorporating Biochar in the Mix

The biochar was sieved and the portion passing the No. 200 sieve was used in the mix as presented in Figure 3.3. The biochar was incorporated into the mix by leaving it in the oven to dry at a temperature of 100 °C. While the biochar was kept in the oven, the asphalt binder was also put in the oven till it reached a temperature of 100 °C.

Figure 3.3: Sieving the Biochar

Afterwards, the biochar was added to the binder and stirred vigorously with a spatula on a hot plate till the binder became smooth while stirring and there was no trace of biochar in

sight. At this point, the biochar had already been evenly incorporated into the mix. Figure 3.4 shows the mixing process.

Figure 3.4: Mixing the Biochar and Asphalt Binder

3.2.2. Batching and Mixing

The first step in the experimental stage entailed determining the tests to be conducted and the number of samples needed to conduct the tests. From the tests sample quantity, it was determined that 60 kg of aggregates having 6% asphalt content by total weight of the mix would be sufficient for testing each batch (keeping in mind that there are five batches in total: the control mix, 5% and 10% biochar by weight of asphalt binder for the two types of biochar). From the mass of 60 kg, the samples were broken down to determine how

many kilograms of each sieve size of each type of aggregate would be used based on the mix design provided by GEMTEC. Table 3.3 shows the blend card used for each 60 kg aggregate batch. From the 60 kg batch, four batches of 15 kg mix were made to foster the easy mixing of the aggregates and the binder in the lab. The aggregates were then sieved and batched using the blend card.

Table 3.3: Aggregate Blend Card

	Gravel (g)	Dirty (g)	Washed (g)	Blend (g)
Ret 12.5	0	0	0	0
Ret 9.5	4884	0	0	0
Ret 6.3	12654	394	185	0
Ret 4.75	3219	2435	949	0
Ret 2.36	888	9397	3032	0
Pass 2.36	555	12374	4234	4800
Total	22200	24600	8400	4800
Virgin AC		6%	3830	
Weight of the mix			60000	
Total weight of the mix			63830	

After batching, the aggregates were quartered in accordance with method B in AASHTO R76 to ensure an even blend. The batched sample was poured on a large plastic bag and turned over several times with the use of a scoop. Then, the sample was heaved into a conical pile, which was flattened into a uniform thickness and diameter until the diameter was approximately four to eight times the thickness of the pile. After the flattening process, the sample was divided into four quarters, as displayed in Figure 3.5. Two diagonally opposite quarters were then merged, and the merged samples were poured into the mixing bucket. The same process was repeated for the other two quarters.

Figure 3.5: Quartering the Sample

The aggregate in the bucket was put in the oven to dry overnight at a temperature of 110°C. The following day, the oven temperature was increased to 148°C. Once the aggregates and the binder reached a temperature of 148°C, the binder was added to the aggregates as seen in Figure 3.6 and mixed quickly till all the aggregates were evenly coated with the asphalt binder.

Figure 3.6: Adding the Binder to the Aggregate and Mixing

3.2.3. Determining Maximum Relative Density (MRD)

Once the asphalt mix was made, the MRD test was conducted on the mixes in accordance with AASHTO T209, Standard Method of Test for Theoretical Maximum Specific Gravity (G_{mm}) and Density of Asphalt Mixtures. 1500 g of sample of the mix was collected after mixing and cooled to room temperature. A flask was put on a scale and tared, the cooled sample was transferred into the flask, and the weight of the sample was recorded. Water at 25 °C was added to the sample in the flask until the sample was fully submerged, then the flask was covered with an airtight vacuum lid.

The flask with the sample and water was placed on a mechanical agitation device connected to a vacuum pump for 15 minutes to remove air from the flask. Afterwards, the vacuum pressure was released, and the sample was extracted from the device. The lid was removed, and the sample was slowly suspended in water with the lid put back on. The covered flask was then taken out of the water, and the body of the flask was dried with a towel to remove excess water. The weight of the sample, flask and water was then recorded and used to calculate the MRD using equation 1.

$$G_{mm} = \frac{A}{A + D - E} \qquad \text{(E. 1)}$$

Where:

G_{mm} = maximum specific gravity of the asphalt mixture,

A = mass of dry sample in air (g),

D = mass of flask and lid filled with water (g),

C = mass of flask, sample and lid filled with water (g).

3.2.4. Compacting the Mix

The mix was compacted in accordance with AASHTO T312, Standard Method of Test for Preparing and Determining the Density of Asphalt Mixture Specimens by Means of the Superpave Gyratory Compactor. The asphalt mix was short term conditioned for 4 hours at 135 °C as specified in AASHTO R30. The compaction mould and base plate were placed in an oven at the compaction temperature of 135 °C.

After the mix was short term conditioned, the sample was left in the oven till it reached the compaction temperature. Then, a paper disc was put in the mould, and the sample was poured into the mould with another paper disc placed over it before the base plate was added. The sample was then compacted in the Superpave gyratory compactor. Figure 3.7 shows the Superpave gyratory compactor used.

Figure 3.7: Superpave Gyratory Compactor

Two sizes of cylinders were compacted: a large and a small one. The large cylinder was used for the dynamic modulus and flow number test, while the small cylinder was used for the fracture energy and flexibility index test. Figure 3.8 shows the small and large cylinders after compaction. Approximately 6140 g of sample was used to compact the large cylinders, and approximately 1887 g of sample was used for the small cylinders. The large cylinder had a height and diameter of approximately 150 mm after compaction. The small cylinder had a height and diameter of approximately 50 mm and 150 mm, respectively, after compaction.

Figure 3.8: Small and Large Cylinders After Compaction

The number of gyrations used for the compaction varied depending on the size of the cylinder and the type of mix compacted. Table 3.4 summarizes the number of gyrations

used for the mix types and cylinder sizes to achieve an air void content of approximately 7 %.

Table 3.4: Number of Gyrations Used for Compacting the Mixes

Mix Type	Number of gyrations	
	small cylinder	large cylinder
Control	65	35
5% Slow pyrolysis biochar	28	20
5% Fast pyrolysis biochar	28	20
10% Slow pyrolysis biochar	28	20
10% Fast pyrolysis biochar	26	16

3.2.5. Determining the Bulk Relative Density and Air Void Content

The bulk specific gravity of the compacted mix was determined in accordance with AASHTO T166, Standard Method of Test for Bulk Specific Gravity (G_{mb}) of compacted Asphalt Mixtures Using Saturated Surface-Dry Specimens. The mass of the cylinder in air is recorded. Afterwards, the cylinder is suspended in water for five minutes, and the weight in water is recorded. The cylinder is then taken out of the water and patted quickly with a towel to remove the excess surface water. The saturated cylinder is then weighed in air. The bulk specific gravity is calculated using equation 2.

$$G_{mb} = \frac{A}{(B - C)} \qquad \text{(E. 2)}$$

Where:

A = mass of the dry specimen in air (g),

B = mass of the saturated surface-dry specimen in air (g),

C = mass of the specimen in water (g).

The air void content of the compacted cylinder was determined using AASHTO T269, Standard Method of Test for Percent Air Voids in Compacted Dense and Open Asphalt Mixtures. The air void content is determined using equation 3.

$$V_a = 100\left(1 - \frac{G_{mb}}{G_{mm}}\right) \quad \text{(E. 3)}$$

Where:

V_a = percent air voids,

G_{mb} = the bulk specific gravity,

G_{mm} = the theoretical maximum specific gravity.

3.3.Dynamic Modulus Test

To evaluate the effect of biochar in the response of the asphalt mix to load, the dynamic modulus test was conducted in accordance with AASHTO T342, Standard Method of Test for Determining Dynamic Modulus of Hot Mix Asphalt (HMA). The large cylinders were cored using a coring drill, as seen in Figure 3.9, to have a diameter between 100 and 104 mm with a standard deviation of 1 mm. The cylinder was then ground to an average height between 147.5 and 152.5 mm, as shown in Figure 3.10. Afterwards, the air void of the cored and ground cylinder was determined and recorded.

Figure 3.9: Coring the Large Cylinders

In total, 30 specimens were cored and ground. The control sample, 5% slow and fast pyrolysis, and 10% slow and fast pyrolysis biochar had six specimens, respectively. Of the six specimens, three were tested for dynamic modulus after short term ageing and compaction. The remaining three specimens were long term aged in accordance with AASHTO R30. The specimens were grouped such that the average air void was similar for the short term aged samples and the long term aged samples. The compacted specimens were conditioned in the oven for 120 hours at a temperature of 85 °C. After conditioning, the samples were tested for dynamic modulus. Fifteen specimens in total were conditioned for long term ageing.

Figure 3.10: Grinding the Large Cylinders

To test for the dynamic modulus, studs were attached to the samples using a quick setting epoxy, JB weld ®, so the sensors could be attached to the specimens. Once the studs were attached, the sensor support jigs were affixed to the studs with the use of screws, as shown in Figure 3.11.

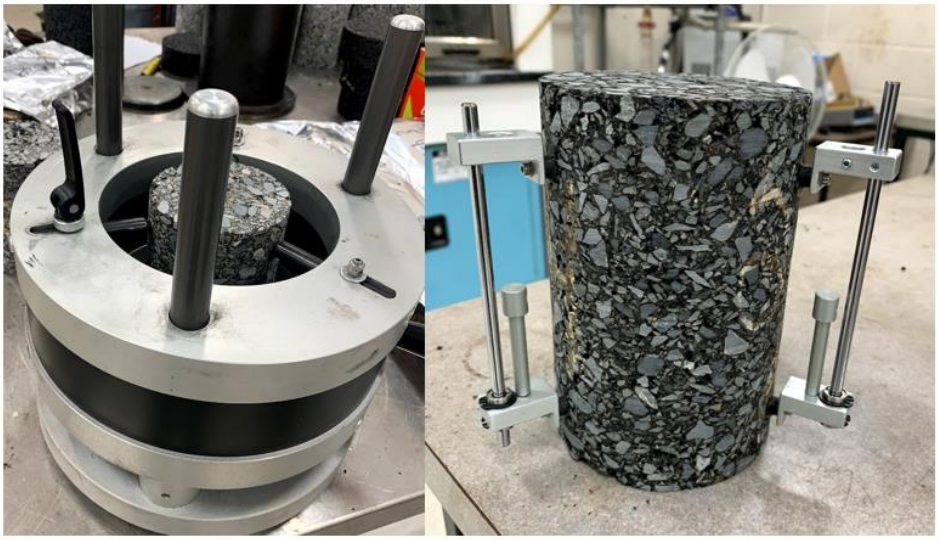

Figure 3.11: Attaching the Studs and Sensor Support Jig to the Specimen

The samples were tested at four temperatures (-10, 4.4, 21.1 and 37.8 °C) and six loading frequencies (0.1, 0.5, 1, 5, 10, 25 Hz) starting each test from the lowest to the highest temperature and the highest to the lowest frequency of loading. As the temperature increased, the more difficult it is to conduct the test. Testing was not conducted at 54 °C because the studs glued to the sample kept coming off at high temperatures as the binder became too soft, making the sensor support jig unstable, so the fifth temperature was omitted. The author of the standard recommended that for PG 58-28, the highest temperature to conduct the dynamic modulus test is 35 °C. The highest temperature reached during testing was 37.8 °C.

The chamber in Figure 3.12 was used to test the specimens. An unconfined test was carried out. Three specimens were tested in the chamber at a time to reduce the conditioning time required for the 30 cylinders. An extra cylinder that had a hole drilled in the center was used to monitor the internal temperature of the samples in the chamber, and once the desired test temperature was reached, the testing was automatically conducted by the servo-hydraulic dynamic testing system (DTS). The proportional gain inputted in the software for temperatures ranging from -10 to 21 °C was 3200, and the proportional gain used for the temperature at 37 °C was 4400. In the dynamic modulus test, as the temperature increases, the modulus reduces. Therefore, the initial expected order of magnitude of the modulus inputted into the software was 20000, 14000, 8000 and 750 MPa for temperatures of -10, 4.4, 21.1, and 37.8 °C, respectively.

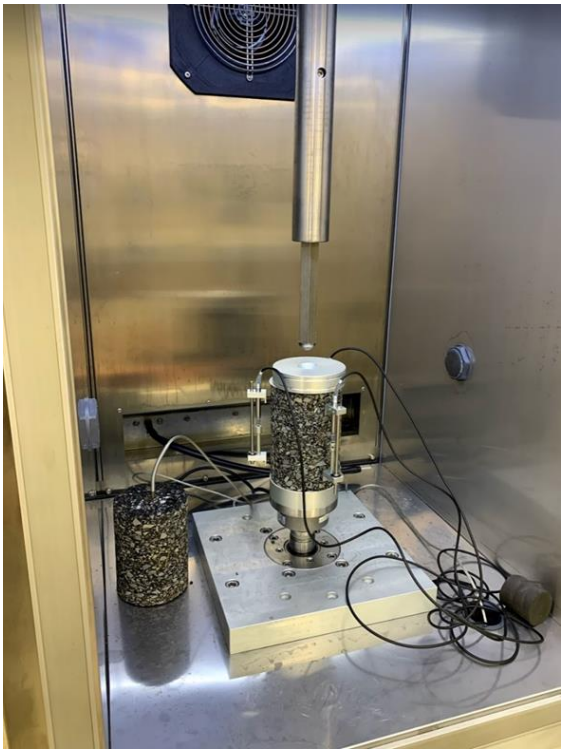

Figure 3.12: Testing Chamber Used for the Dynamic Modulus and Flow Number Test

After the test was conducted, the data was extracted from the software and AASHTO R62, Standard Practice for Developing Dynamic Modulus Mater Curves for Asphalt Mixtures, was used to analyze the test results. The standard presents the general form of the dynamic modulus master curve equation, which is a sigmoid function included in the Mechanistic-Empirical Pavement Design Guide (MEPDG), as presented in equation 4.

$$\log|E^*| = \delta + \frac{(\alpha)}{1 + e^{\beta+\gamma log f_r}} \quad \text{(E. 4)}$$

Where:

|E*| = the dynamic modulus (psi),

α, β, δ, & γ = the fitting parameters,

f_r = the reduced frequency.

The reduced frequency is the computed frequency at the reference temperature, equivalent to the actual loading frequency at the test temperature, and it is computed using time-temperature shift factors. The shift factor represents the shift in frequency associated with a shift from a test temperature to the reference temperature. There are several time-temperature shift functions available, the one used in this study was the second-order polynomial. The second-order polynomial is given in equation 5.

$$\log f_r = \log f + a_1(T_R - T) + a_2(T_R - T)^2 \quad \text{(E. 5)}$$

Where:

f_r = the reduced frequency at the reference temperature,

f = the loading frequency at the test temperature,

a_1, a_2 = the fitting coefficients,

T_R = the reference temperature (°C),

T= the test temperature (°C).

The reference temperature, T_R, used to construct the master curve was 21.1 °C. The final form of the dynamic modulus master curve equation was obtained by substituting the shift factor relation in equation 4 into equation 5. The final form of the equation is given in equation 6.

$$\log|\hat{E}^*| = \delta + \frac{(\alpha)}{1 + e^{\beta+\gamma[\log f + a_1(T_R - T) + a_2(T_R - T)^2}} \quad \text{(E. 6)}$$

The fitting parameters were optimized using the solver function in Microsoft Excel by minimizing the sum of the squared error through varying the fitting parameters. The master curve was then developed by plotting the log of the reduced frequency against the dynamic modulus.

3.4.Flow Number Test

The flow number (FN) is the load cycle at which the rate of change of permanent strain reaches the minimum value. It indicates the start of tertiary flow in asphalt mixtures (Shen and Yu, 2011). FN is a property related to the resistance of asphalt mixtures to permanent deformation (rutting). The flow number test is a destructive test (Roy et al., 2015). A higher flow number means higher rutting resistance (Carter et al., 2018). The flow number test is a repeated load test where a compressive load pulse of 0.1 seconds is applied by a 0.9 second rest period. The temperature used for the flow number test will vary for different locations, and depending on the year the test is conducted, the test temperature will also vary, this is because one of the parameters for determining the test temperature is the project location climatic data obtained from the nearest weather station.

The specimens used for the dynamic modulus test were also used for the flow number test. AASHTO T378-17, which is a "Standard Method of Test for Determining Dynamic Modulus and Flow Number for Asphalt Mixtures Using the Asphalt Mixture Performance Tester (AMPT)," was used to test the specimens. The samples used for the flow number test had dimensions of approximately 100-mm diameter by 150-mm height. The flow number test of the samples was conducted at 58 °C. The test temperature was obtained from the high adjusted PG temperature in Appendix A, Figure A. 2, according to the instructions in Appendix X2.3 of AASHTO T378 using LTPPBind online, available at the U.S Department of Transportation Federal Highway Administration's website (LTPP InfoPave - LTPPBind Online, 2021).

The parameters used to determine the test temperature is listed in Table 3.5. The project location used to get the climatic data from the nearest weather station was Fredericton, New Brunswick.

Table 3.5: Temperature Evaluation Parameters for LTPPBind (AASHTO T378)

Evaluation Parameter		HMA and WMA
Desired reliability, %		50
Target rut depth, mm		12.5
Adjustment for traffic loading and speed		0.0
Depth of layer, mm	Surface layers	20
	Intermediate and base layers	Depth at the surface of the layer

The same testing chamber used for the dynamic modulus test was used for the flow number test. However, the setup in the chamber was different. Transducer sensors were not used for the flow number test. Once the specimens were conditioned to the test temperature, the samples were automatically tested using the servo-hydraulic dynamic testing system. The parameters inputted into the software to conduct the test are listed in Table 3.6. After the test was conducted, the flow number was obtained by identifying the number of cycles where the minimum rate of change of permanent axial strain occurred.

Table 3.6: Flow Number Test Parameters (AASHTO T378)

Test Parameter	**Value**
Test temperature	Adjusted PG temperature (which was 58 °C)
Repeated axial stress	600 kPa
Contact stress	30 kPa
Confining stress	0 kPa (unconfined)

After the test was conducted, the flow number was obtained by identifying the number of cycles where the minimum rate of change of permanent axial strain occurred.

3.5.Fracture Energy and Flexibility Index Test

AASHTO TP124 standard covers the instructions for determining the first mode fracture resistance property of an asphalt mix at intermediate temperatures. This first mode is the tensile opening mode during crack propagation. The small cylinders having an average height of 50 mm and an average diameter of 150 mm were used for the FI test. The cylinders were cut in half, and a notch was sawn on the flat side of the semicircular specimen opposite the curved edge, as shown in Figure 3.13.

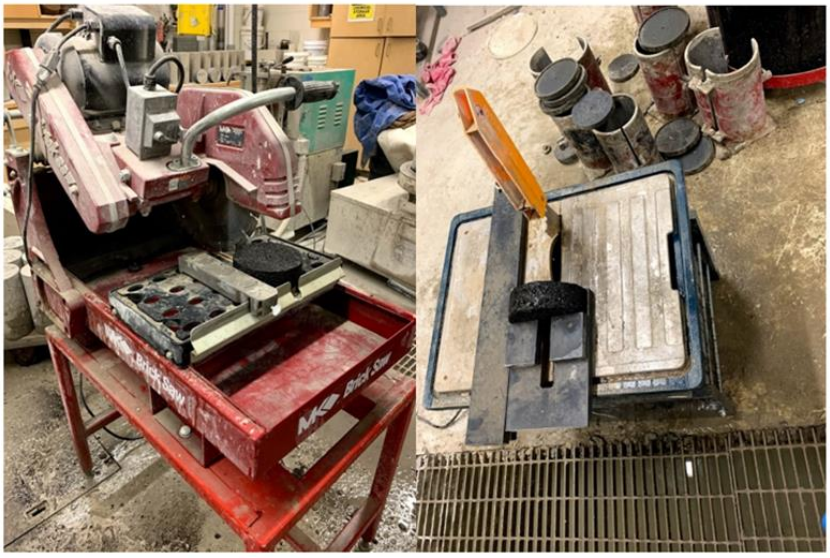

Figure 3.13: Halving and Notching the Small Cylinders

In total, fifteen cylinders were halved to yield thirty semicircular samples. The control sample, 5% slow and fast pyrolysis, and 10% slow and fast pyrolysis biochar had six specimens, respectively. Of the six specimens, three were tested for fracture energy after short term ageing and compaction. The remaining three specimens were conditioned with a single freeze-thaw cycle in accordance with AASHTO T283, Standard Method of Test for Resistance of Compacted Asphalt Mixtures to Moisture-Induced Damage. The

specimens were grouped such that the average air void was similar for the un-conditioned samples and the moisture conditioned sample.

The specimens to be moisture conditioned were placed in a vacuum container filled with water at room temperature. Vacuum was then applied to the specimen for about a minute. The specimens were saturated to achieve a degree of saturation between 70 and 80 percent. Afterwards, the samples were covered tightly with saran wrap and placed in a plastic bag with 10 mL of water and sealed. The sealed bags were put in a freezer at a temperature of -18 °C, for a minimum of 16 hours. Next, the specimens were placed in a water bath at 60 °C for 24 hours and another water bath at 25 °C for 2 hours before conducting the FI test.

For the FI test, the specimens were placed centered on two rollers in the fixture with the notched side down. A load was then applied along the vertical radius of the specimen. The load and line displacement (LLD) were measured all through the test period. Figure 3.14 shows the FI test setup.

Figure 3.14: FI Test Setup

Figure 3.15 presents the specimens before and after testing. After the FI test was conducted, the load and line displacement data were generated from the results.

Figure 3.15: Samples Before and After the FI Test

From the LLD plot, the post-peak slope was obtained and used to determine the fracture energy and flexibility index using equations 7 and 8, respectively.

$$G_{f=\frac{W_f}{Area_{lig}}*10^6} \quad \text{(E. 7)}$$

Where:

G_f = fracture energy,

W_f = work of fracture,

$Area_{lig}$ = ligament area

The area of the ligament was calculated by subtracting the specimen radius from the notch length and multiplying the value by the specimen thickness.

$$FI = \frac{G_f}{|m|} * A \quad \text{(E. 8)}$$

Where:

m = post-peak slope obtained from the graph,

A = a constant value of 0.01.

4. RESULTS AND DISCUSSION

4.1.Effect of Biochar on the Workability of the Asphalt Mixtures

The compaction effort (number of gyrations) required to achieve a target air void content of approximately 7% was used to indirectly analyze whether the addition of biochar improved the workability of the asphalt mixtures.

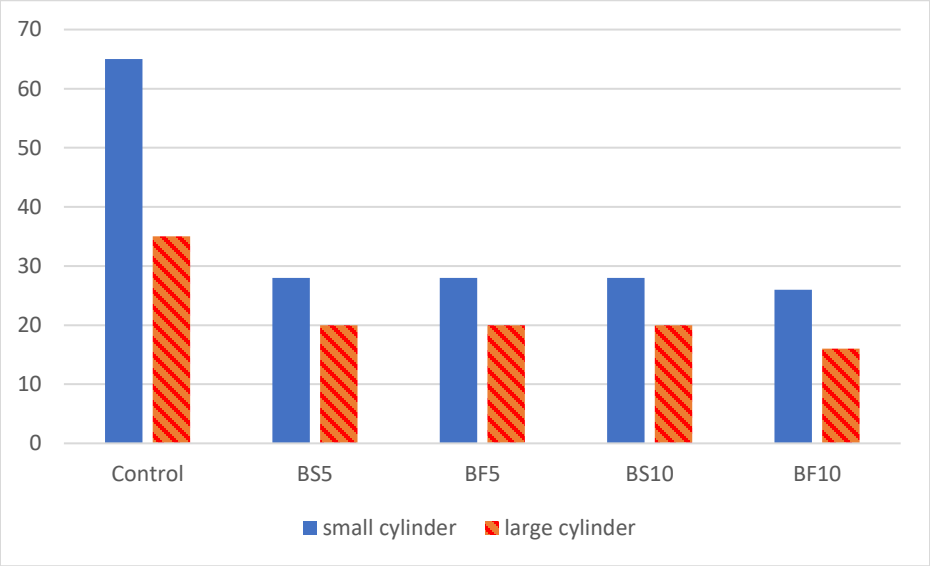

Figure 4.1: Number of Gyrations Used to Compact the Small and Large Cylinders

From Figure 4.1, it can be observed that the addition of biochar to the mix helped reduce the number of gyrations required to achieve the target air void content by a minimum of 43%. The larger cylinders also required a fewer number of gyrations for compaction compared to the smaller cylinders. It is important to note that during the sample preparation, the problem encountered with the mixes was the inconsistency in the air void result after compacting, coring the large samples and halving the small samples. So, the same batch of material compacted at the same weight, temperature and number of gyrations

did not yield the same air void content result. The standard deviation in the air void result of the samples was higher than expected, which might have affected the results.

The air voids variation for the small and large samples is presented in Figure 4.2. The average desired air void content for the large samples mix was 7 ± 0.5%; however, it was difficult to achieve during compaction. As observed in Figure 4.2, only the 5% fast biochar mix met the average desired air void target, with the control samples' air void content being below the desired percentage of air void content and the rest of the mix being above the target range for the large samples. The average desired target air void for the small samples mix was 7 ± 1%, which was not too difficult to achieve; however, some specimens fell below the desired target air void content.

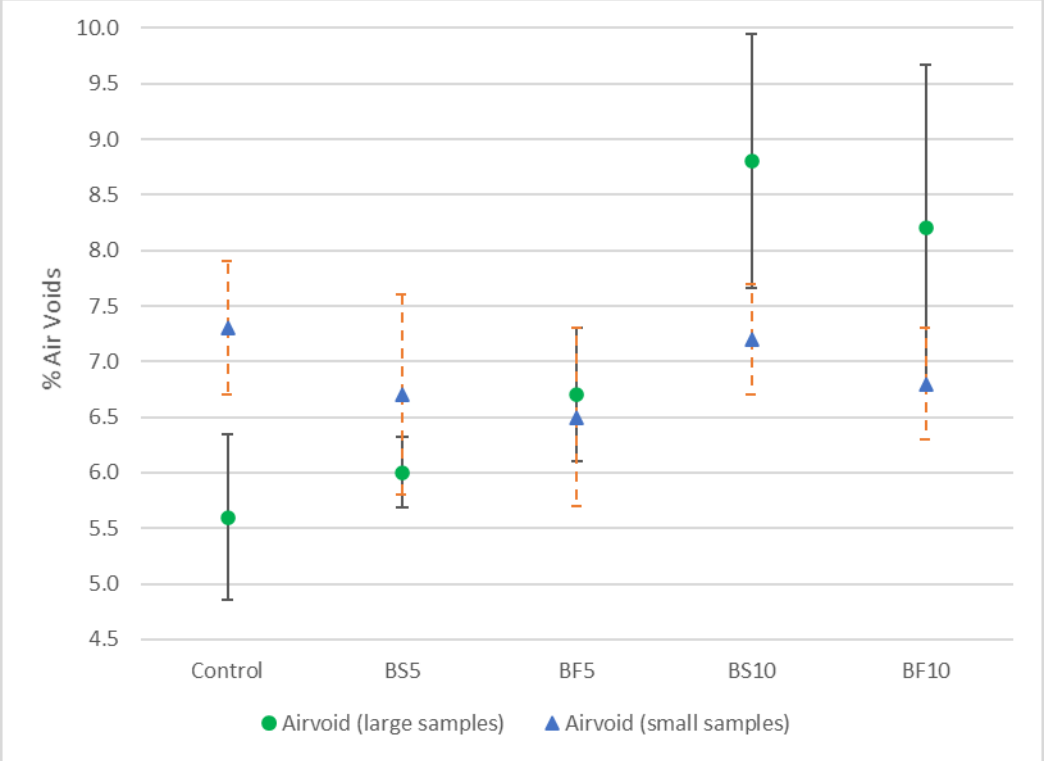

Figure 4.2: Variation in the Air Void Content of the Mix

4.2.Effect of Biochar on the Response of Asphalt Mixtures

This section interprets the result obtained from the dynamic modulus test to determine the effect of biochar on the response of asphalt mixtures to temperature and the frequency of loading on the susceptibility of the asphalt mixture to thermal cracking, fatigue cracking and rutting. The dynamic modulus test data, fitting parameters and master curves supporting this section are presented in Appendix B.

4.2.1. Dynamic Modulus After Short Term Ageing

Figure 4.3 shows the plot of the dynamic modulus master curve after short term ageing of the mix. From the result, the stiffness at different temperatures and frequencies was used as an indicator of the surface distresses in asphalt pavements. From Figure 4.3, it is observed that the 10% slow pyrolysis biochar exhibited lower elastic modulus compared to all other mixtures at low and intermediate frequencies, while the 5% slow pyrolysis biochar exhibited lower elastic modulus at high frequencies. To determine the thermal cracking potential of the asphalt mixtures, the stiffness of the mix was evaluated at a low temperature of -10 °C and a high frequency of 25 Hz (Varamini et al., 2017). A low temperature and high frequency were chosen because it would be the most extreme condition for thermal cracking to occur.

The short term aged dynamic modulus values in Table 4.1 indicate that the 5% slow pyrolysis biochar mix had the lowest stiffness at the high frequency of 25 Hz, which suggests that the mix might have a better thermal cracking resistance. The 5% fast pyrolysis biochar mix had the highest dynamic modulus followed by the control sample, 10% slow, 10% fast and 5% slow pyrolysis biochar mix accordingly. The higher the dynamic

modulus, the stiffer the mix is. When the mix is stiffer, it becomes more brittle and is prone to thermal cracking. So, the worst mix for resisting thermal cracking would be the 5% fast pyrolysis biochar modified mix, and the best mix for resisting thermal cracking would be the 5% slow pyrolysis biochar mix.

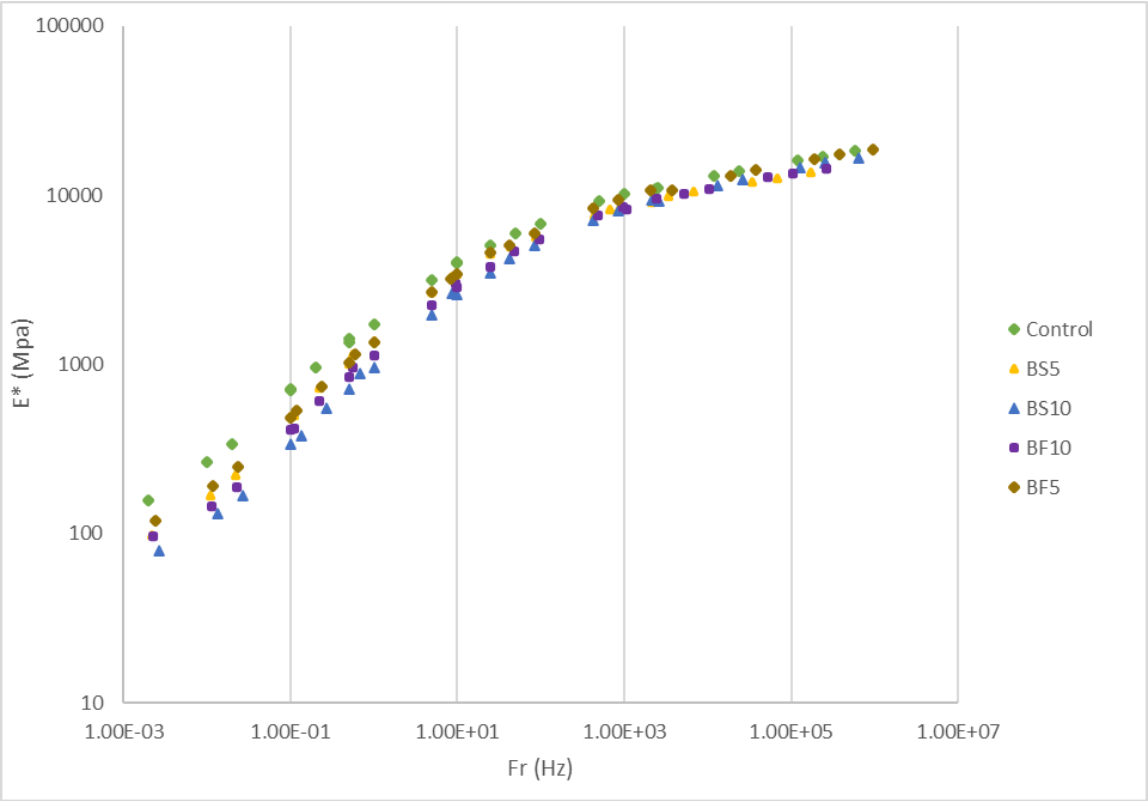

Figure 4.3: Dynamic Modulus Master Curve After Short Term Ageing

Table 4.1: Dynamic Modulus of the Asphalt Mixtures After Short Term Ageing

Mix Type	Dynamic Modulus, E* (MPa)		
	-10 °C & 25 Hz	21.1 °C & 10 Hz	37.8 °C & 0.1 Hz
Control	18220	3932	158
BS5	13563	3411	98
BF5	18643	3395	120
BS10	16615	2575	79
BF10	14370	2836	96

A mix that is too stiff can result in fatigue cracking and thermal cracking, which are major distresses in asphalt pavements (Rahbar-Rastegar et al., 2018). To determine the fatigue cracking potential of the asphalt mixtures, the stiffness of the mix was evaluated at a temperature of 21.1 ℃ and an intermediate frequency of 10 Hz (Varamini et al., 2017), as it is the most extreme condition for fatigue cracking to occur. The dynamic modulus value of the short term aged samples in Table 4.1 indicates that the 10% slow pyrolysis biochar mix had the lowest stiffness at an intermediate frequency of 10Hz, which suggests that the mix might have improved the fatigue cracking resistance level of the mix. The control mix had the highest dynamic modulus followed by the 5% slow, 5% fast, 10% fast, and 10% slow pyrolysis biochar mix accordingly. The higher the dynamic modulus, the stiffer the mix is. When the mix is stiffer, it becomes more brittle and is prone to fatigue cracking. So, the worst mix for resisting fatigue cracking in this case would be the control mix and the best mix for resisting fatigue cracking would be the 10% slow pyrolysis biochar mix.

To determine the rutting potential of the asphalt mixtures, the stiffness of the mix should be evaluated at a high temperature of 54.4 ℃ and a low frequency of 0.1 Hz (Varamini et al., 2017), as it is the most extreme condition for rutting to occur. While testing, it was difficult to conduct the dynamic modulus test at 54.4 ℃ as the PG 58-28 asphalt binder became too soft, so the sensor support jig was not stable. The equipment manufacturer recommended 35 ℃ as the highest test temperature for the asphalt binder performance grade. The rutting susceptibility can be evaluated at a temperature of 38 ℃ (Apeagyei, 2011). The highest temperature reached during testing was 37.8 ℃, and the flow number test results would be relied upon to support the findings. As presented in Table 4.1, the control mix had the highest dynamic modulus, followed by the 5% fast, 5% slow, 10% fast,

and 10% slow pyrolysis biochar mix accordingly. The higher the dynamic modulus, the stiffer the mix is. When the mix is stiffer, it becomes more resistant to rutting. So, the worst mix for rutting resistance, in this case, would be the 10% slow pyrolysis biochar mix, and the best mix would be the control mix. The lower stiffness of the 10% slow pyrolysis biochar at the low frequency of 0.1 Hz might suggest a lower level of rutting resistance for the mix after short term ageing.

4.2.2. Dynamic Modulus After Long Term Ageing

Figure 4.4 shows the plot of the dynamic modulus master curve after long term ageing of the mixtures. From the dynamic modulus results, the stiffness at different temperatures and frequencies were used as indicators of the surface distresses in asphalt pavements. From Figure 4.4, it is observed that the 10% fast pyrolysis biochar exhibited lower elastic modulus compared to all other mixtures at low frequencies and the 10% slow pyrolysis biochar exhibited lower elastic modulus at high and intermediate frequencies when compared with other mixes.

The stiffness of the mix after long term ageing was also evaluated at a low temperature of -10 °C and a high frequency of 25 Hz to determine the thermal cracking potential of the asphalt mixtures (Varamini et al., 2017). Table 4.2 shows the dynamic modulus results for the long term aged samples at the specified temperature and frequency. The long term aged dynamic modulus values in Table 4.2 indicate that the 10% slow pyrolysis biochar mix had the lowest stiffness at the high frequency of 25 Hz, which might suggest that the mix might have a better thermal cracking resistance. The 5% slow pyrolysis biochar seemed to have a better thermal cracking resistance after short term ageing.

From Table 4.2, the 5% fast pyrolysis biochar mix had the highest dynamic modulus after long term ageing, followed by the 5% slow pyrolysis biochar mix, control mix, 10% fast and 10% slow pyrolysis biochar mix accordingly. The worst mix for resisting thermal cracking, in this case, would be the 5% fast pyrolysis biochar modified mix, and the best mix for resisting thermal cracking after long term ageing would be the 10 % slow pyrolysis biochar mix.

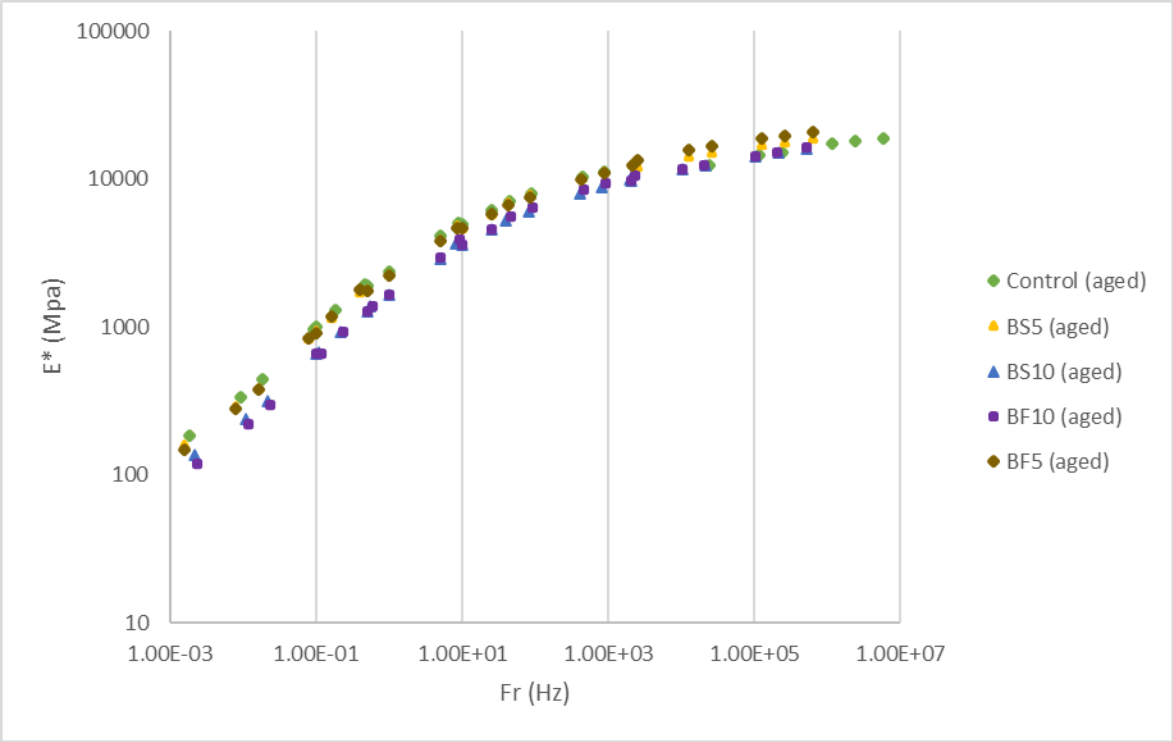

Figure 4.4: Dynamic Modulus Master Curve after Long Term Ageing

The stiffness of the asphalt mixtures after long term ageing was also evaluated at a temperature of 21.1 °C and an intermediate frequency of 10 Hz to determine the fatigue cracking potential of the mix (Varamini et al., 2017). Table 4.2 shows the dynamic modulus results for the long term aged samples at the specified temperature and frequency. The long term aged dynamic modulus value in Table 4.2 indicates that the 10% slow pyrolysis

biochar mix had the lowest stiffness at an intermediate frequency of 10 Hz, which suggests that the mix might have improved the fatigue cracking resistance level of the mix. The 10% slow pyrolysis biochar also seemed to have a better resistance to fatigue cracking after short term ageing.

Table 4.2: Dynamic Modulus of the Asphalt Mixtures After Long Term Ageing

Mix Type	Dynamic Modulus, E^* (MPa)		
	-10 °C & 25 Hz	**21.1 °C & 10 Hz**	**37.8 °C & 0.1 Hz**
Control	18925	4961	185
BS5	19022	4695	160
BF5	20977	4666	148
BS10	16098	3607	136
BF10	16459	3621	120

From Table 4.2, the control mix had the highest dynamic modulus followed by the 5% slow, 5% fast, 10% fast, and 10% slow pyrolysis biochar mix after long term ageing accordingly. The higher the dynamic modulus, the stiffer the mix is, which leads to a brittle mix that is more susceptible to fatigue cracking. The worst mix for resisting fatigue cracking after long term ageing would be the control mix, and the best mix for resisting fatigue cracking would be the 10% slow pyrolysis biochar mix.

To determine the rutting potential of the asphalt mixtures, the stiffness of the mix was also evaluated at a high temperature of 37.8 °C and a low frequency of 0.1 Hz. The flow number test results would be used to back up the findings in Table 4.2, which shows the dynamic modulus results for the long term aged samples at 37.8 °C and 0.1 Hz. The long term aged dynamic modulus value in Table 4.2 indicates that the control mix had the highest dynamic modulus followed by the 5% slow, 5% fast, 10% slow, and 10% fast pyrolysis biochar mix after long term ageing accordingly. The higher the dynamic modulus, the stiffer the mix is.

When the mix is stiffer, it becomes more resistant to rutting. So, the worst mix for rutting resistance, in this case, would be the 10% fast pyrolysis biochar mix, and the best mix would be the control mix. Before long term ageing, the worst mix for resisting rutting was the 10% slow pyrolysis biochar, but the control mix still remained the best mix that seems to resist rutting before and after long term ageing. The lower stiffness of the 10% fast pyrolysis biochar at the low frequency of 0.1 Hz might suggest a lower level of rutting resistance for the mix after long term ageing.

4.2.3. Effect of Ageing on the Mixes Response

From Table 4.3, it is observed that the addition of biochar might make the mix more susceptible to ageing, as the percent change in dynamic modulus for the biochar added mixes are higher than that of the control mix, except for the 10% slow pyrolysis biochar which made the mix less stiff at lower temperatures. The reduction in stiffness of the 10% slow pyrolysis biochar mix after long-term ageing might be a result of errors during testing, so it can be considered as an outlier. The hypothesis stated that the addition of biochar reduced the ageing susceptibility of the mix; however, that is not the case. The addition of biochar seems to increase the ageing susceptibility of the mix.

Table 4.3: Effect of Long Term Ageing on the Stiffness of the Mix

Mix Type	Percent Change in Dynamic Modulus, E^*		
	-10 °C & 25 Hz	21.1 °C & 10 Hz	37.8 °C & 0.1 Hz
Control	4%	26%	17%
BS5	40%	38%	63%
BF5	13%	37%	23%
BS10	-3%	40%	72%
BF10	15%	28%	25%

Table 4.3 indicates at lower temperatures that as the samples age, the stiffness of the sample increases, with an exception to the 10% slow pyrolysis biochar. The increase in stiffness after long term ageing means the mixes are more prone to thermal cracking over time at low temperatures, which is expected. The 5% slow pyrolysis biochar mix had the greatest increase in stiffness after ageing at low temperatures. It seems that the long term ageing of the mix improved the thermal cracking resistance of the 10% slow pyrolysis biochar mix at -10 °C.

It can also be observed in Table 4.3 that the stiffness of the mixes at intermediate temperatures increased after long term ageing, which is expected to happen. The increase in stiffness after long term ageing indicates that the mixes are more prone to fatigue cracking over time. The 10% slow pyrolysis biochar mix had the highest increase in stiffness after long term ageing at 21.1 °C**.**

It is observed in Table 4.3 that long term ageing increased the dynamic modulus of the mixes at high temperatures. This means the mixtures became stiffer, thereby making them more resistant to rutting. The 10% slow pyrolysis biochar mix had the highest increase in stiffness after long term ageing at 37.8 °C**.**

4.3.Effect of Biochar on the Rutting Resistance of Asphalt Mixture

This section explains the flow number results obtained from the tests for both the short term aged and long term aged samples. Typically, a higher flow number value means the mix has a higher rutting resistance, which makes the mix less prone to permanent deformation. The test data for the results in this section is provided in Appendix C.

4.3.1. Flow Number After Short Term Ageing

Figure 4.5 shows the flow number test results of the short term aged asphalt mixtures. From the test result in Figure 4.5, it is observed that the flow number after short term ageing decreased with the addition of biochar, which means the mixes containing biochar exhibit tertiary flow earlier and are more prone to rutting. The increase in the biochar content further increased the rutting potential of the mix. It is important to note that biochar was used as a filler, so there was no change in the asphalt content; this, in turn, could be lubricating the mix and facilitating the mobility of the aggregates at high temperatures.

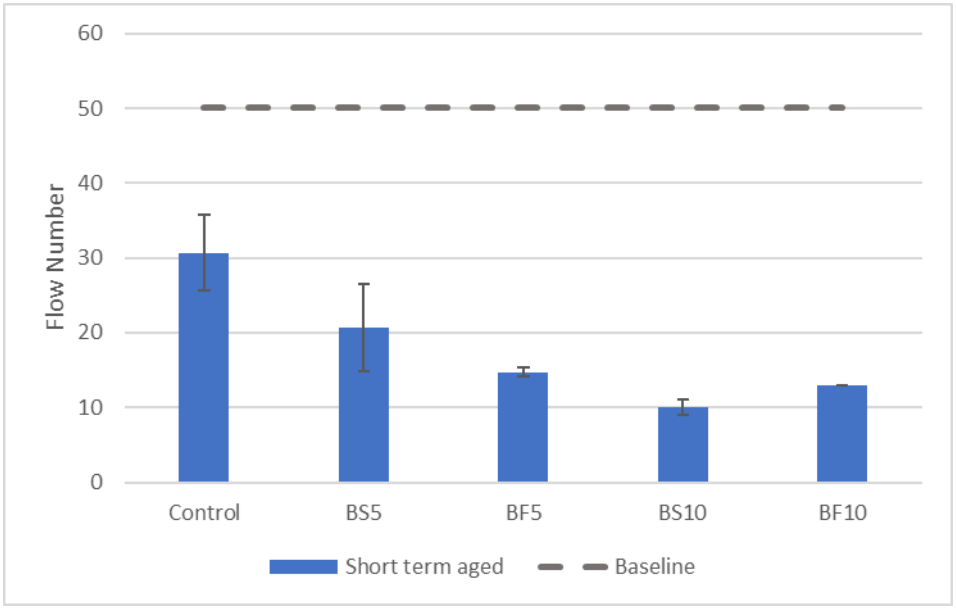

Figure 4.5: Flow Number of the Asphalt Mixtures After Short Term Ageing

It was expected that the mixes had a flow number above 50 for a traffic level between 3 to <10 million ESALs according to AASHTO T 378, but this was not achieved for the control mix and the biochar modified mixes. It is not uncommon to have flow number values below 50. It appears that the flow number test results obtained might be suitable for traffic levels less than 3 million ESALs as the standard does not specify any value for that traffic level.

It is important to note that the flow number decreases with an increase in air voids (Yu et al., 2012). The difference in air void could be a factor to consider apart from the biochar content in the flow number result. There is a 33%, 52%, 67% and 58% difference in the flow number between the control sample and the 5% slow, 5% fast, 10% slow and 10% fast pyrolysis biochar, respectively. From the dynamic modulus master curve, it was observed that the control sample seems to be the best mix for resisting rutting, which is confirmed in the flow number test results, as the control sample had the highest flow number after short term ageing.

4.3.2. Flow Number After Long Term Ageing

Figure 4.6 indicates that the addition of biochar still resulted in a decrease in the flow number when compared with the control mix except for the 5% fast pyrolysis biochar. The decrease in the flow number due to the biochar content might result in an increase in the rutting potential of the mixes. The 5% fast pyrolysis biochar was a unique case since it experienced a 60% increase in the flow number compared to the control sample after long term ageing, which is higher than expected. There seems to have been an anomaly during testing for the 5% fast pyrolysis biochar mix to yield the 60% increase in flow number. The result from the 5% fast pyrolysis is considered an outlier. Therefore, the control sample remains the most favorable mix for addressing the rutting susceptibility of the asphalt mixtures even after long term ageing.

It appears that the flow number test results obtained might be suitable for traffic levels less than 3 million ESALs except for the 5% fast pyrolysis biochar mix, which has a flow number suitable for a traffic level between 3 to <10 million ESALs. There is a 26%, 60%,

52% and 39% difference in the flow number between the control sample and the 5% slow, 5% fast, 10% slow and 10% fast pyrolysis biochar after long term ageing, respectively.

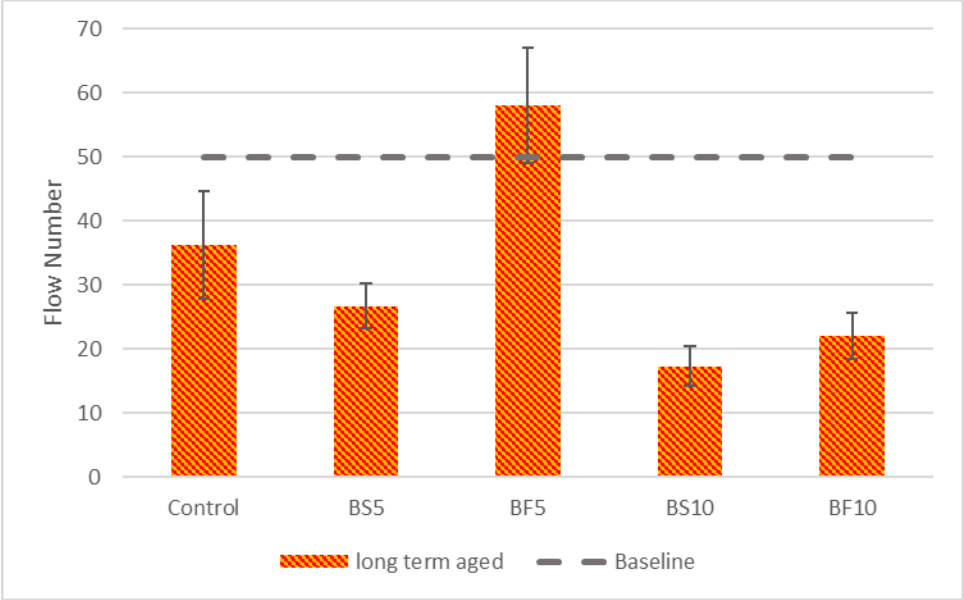

Figure 4.6: Flow Number of the Asphalt Mixtures After Long Term Ageing

4.3.3. Effect of Ageing in Rutting Susceptibility

From the test result in Table 4.4, it is observed that the flow number of the samples increased after long term ageing, which corresponds to the increase in the dynamic modulus of the samples after long term ageing described in section 4.2.3.

Table 4.4: Change in the Flow Number After Long Term Ageing

Mix Type	Percent change in Flow number
Control	18%
BS5	29%
BF5	295%
BS10	73%
BF10	27%

The flow number of the 5% fast pyrolysis biochar was almost tripled after long term ageing when compared to the short term aged sample. The rate of increase seems suspicious; nonetheless, all the three samples tested had a similarly high result. A possible reason for this could be that the temperature at the time of the test was unintentionally below the target. A retest would have been done; however, the mix available was not enough to conduct another test. For that reason, the result is considered an outlier. From Table 4.4, it is observed that the addition of biochar to the mix makes the mix more susceptible to ageing.

4.4. Effect of Biochar on the Fatigue Cracking Resistance of Asphalt Mixtures

This section explains the effect of biochar on the fatigue cracking resistance of the asphalt mixtures using the fracture energy and the flexibility index, as well as the effect of moisture damage on the fracture energy and flexibility index of the asphalt mixtures. The data supporting this section is presented in Appendix D.

4.4.1. Fracture Energy and Flexibility Index of Unconditioned Samples

Figure 4.7 presents the results for the unconditioned mixtures. Figure 4.7 indicates that the 10% fast pyrolysis biochar had the least detrimental effect on the FI value of the asphalt mixture. There is a 53%, 33%, 19% and 12% difference in the flexibility index between the control sample and the 5% slow, 5% fast, 10% slow and 10% fast pyrolysis biochar, respectively. In Figure 4.7, it can be observed that the flexibility index seems to increase with the increase in the percentage of biochar, so 10% biochar added mixes had higher FI values compared to the 5% biochar added mixes. The increase in FI yields an improvement

in cracking resistance, which supports the finding from the dynamic modulus test results that adding biochar at the higher content of 10% is beneficial for improving the resistance to cracking of the mix.

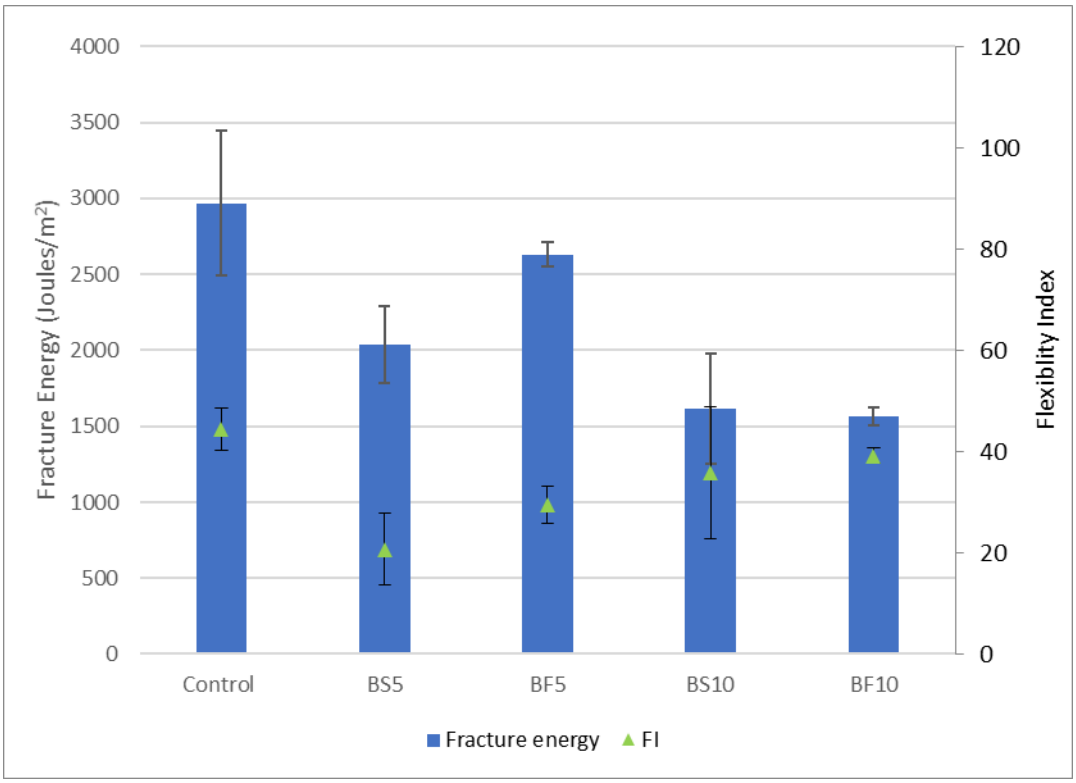

Figure 4.7: Fracture Energy and Flexibility Index Before Conditioning

From the dynamic modulus result, it was suggested that the 10% slow pyrolysis biochar was preferable for resisting fatigue cracking, while the control mix was the least preferable mix to help resist fatigue cracking. However, the results of the FI test suggest that the control mix is preferred for fatigue cracking resistance. These variations in the test results can be attributed to several factors. One of the reasons for the variation is that the test procedure conducted is different. The compaction effort and the sample size used for both tests are different. Also, the air void content of the specimens used for the dynamic modulus

and flow number test were not within the target range, while the air void content of the samples used for the FI test was within and/or closer to the target range of 6 to 8%.

The 5% fast pyrolysis biochar mix had the lowest fracture energy. There is a 31%, 11%, 46% and 47% reduction in the fracture energy between the control sample and the 5% slow, 5% fast, 10% slow and 10% fast pyrolysis biochar mix, respectively.

4.4.2. Fracture Energy and Flexibility Index of Conditioned Samples

Figure 4.8 shows the results for the mixtures conditioned with a single freeze-thaw cycle.

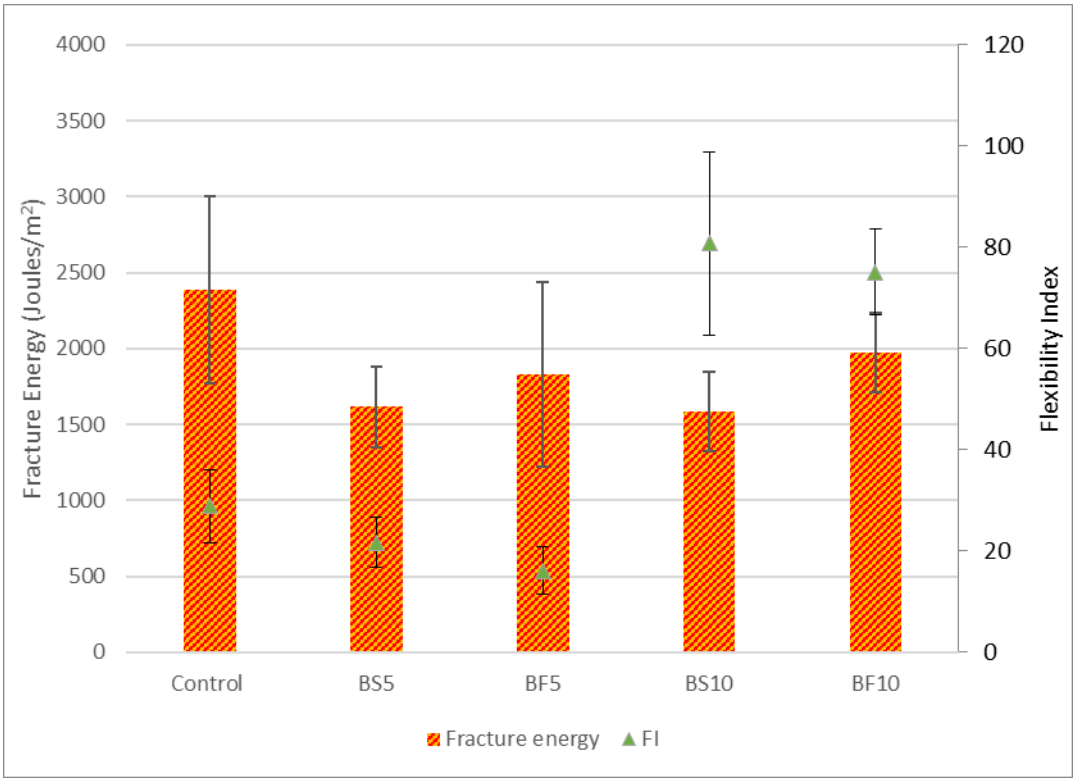

Figure 4.8: Fracture Energy and Flexibility Index After Moisture Conditioning

From the control mix, 5% biochar and the 10% slow pyrolysis biochar mix, it is observed in Figure 4.8 that the fracture energy of the asphalt mixture decreased after moisture conditioning, which is expected as the conditioned asphalt mixtures have incurred moisture

damage from the single freeze-thaw cycle applied. Since the mixture has experienced moisture damage, the cracking potential of the mixture is greater.

From the conditioned samples in Figure 4.8, it is observed that the 10% slow pyrolysis had the highest FI value, which means it is the preferable mix for resisting cracking.

The control sample had the highest fracture energy, while the 10% slow pyrolysis biochar had the lowest fracture energy of the mixture compared to the other biochar added mixes. There is a 32%, 23%, 34% and 17% reduction in the fracture energy between the control sample and the 5% slow, 5% fast, 10% slow and 10% fast pyrolysis biochar, respectively for the conditioned samples.

There is a 25% decrease, 44% decrease, 180% increase and 160% increase in the flexibility index between the control sample and the 5% slow, 5% fast, 10% slow and 10% fast pyrolysis biochar, respectively, after moisture conditioning. In Figure 4.5, it can be observed that the flexibility index increased with the increase in the percentage of biochar, so 10% biochar added mixes had higher FI values compared to the 5% biochar added mixes after moisture conditioning. The increase in FI yields an improvement in cracking resistance.

4.4.3. Effect of Moisture on the Fatigue Cracking Susceptibility of the Mix

Table 4.5 shows the 10% fast pyrolysis biochar mix having a 26% increase in the fracture energy after moisture conditioning, and the rest of the samples had a reduced fracture energy after moisture conditioning.

Table 4.5: Effect of Moisture on the Cracking Potential of the Mixes

Mix Type	Percent Change after Conditioning	
	Fracture Energy	**Flexibility Index**
Control	-20%	-35%
BS5	-21%	5%
BF5	-30%	-45%
BS10	-2%	126%
BF10	26%	92%

It can also be observed that the 10% biochar content mixes significantly increased the FI after moisture conditioning, which might suggest that the 10% biochar content mixes resist cracking more efficiently after moisture conditioning.

5. CONCLUSION AND RECOMMENDATIONS

Two types of biochar were tested at five and ten percentage by weight of asphalt binder. The dynamic modulus test results of the samples were used to determine the rutting, fatigue cracking and thermal cracking resistance of the mix. The flow number and flexibility index test were carried out to support the findings from the dynamic modulus test results. The study also considered the effect of biochar on the workability, susceptibility to ageing and effect of moisture damage on the mix. The findings from the result are summarized below, and it is important to note that the variation in the air void content of the asphalt mixtures could have affected the results of the study.

5.1.Conclusions

The compaction effort was used to indirectly determine whether the addition of biochar improved the workability of the mix. By comparing the compaction effort for the mixes, the addition of biochar seemed to improve the workability of the mix. The mixes containing biochar required a fewer number of gyrations to achieve the same air void content. The number of gyrations required to compact the samples with biochar reduced by at least 43%, which might help save time and effort in the field during paving in asphalt roadway construction. The hypothesis that biochar improves the workability of the mix seems to be true.

From the tests conducted on the response of asphalt mixtures to temperature and frequency of loading before and after long term ageing, the findings are summarized below:

- The 5 % slow pyrolysis biochar mix seemed to have the best thermal cracking resistance after short term ageing, while the 10% slow pyrolysis biochar mix

seemed to have a better thermal cracking resistance after long term ageing. The worst mix for the thermal cracking resistance of the mix was the 5% fast pyrolysis biochar mix before and after long term ageing.

- The 10% slow pyrolysis biochar might have improved the fatigue cracking resistance of the mix before and after long term ageing at an intermediate frequency of 10 Hz. The mix with the least fatigue cracking resistance ability was the control mix before and after long term ageing. So, the addition of biochar seemed to improve the fatigue cracking resistance of the mix.
- The control mix seemed to perform best in addressing the rutting susceptibility of the mix before and after long term ageing at a low frequency of 0.1 Hz. The 10% slow pyrolysis biochar mix seemed to be the least performing mix in addressing the performance of the mix to rutting after short term ageing, while the 10% fast pyrolysis biochar mix was the worst after long term ageing. So, the addition of biochar seemed to compromise the rutting resistance of the mix.
- It was hypothesized that the addition of biochar to the mix would help reduce the susceptibility of the mix to ageing. However, that was not the case. The addition of biochar seemed to increase the susceptibility of the mix to ageing. Therefore, biochar used as a filler does not enhance the resistance of the mix to ageing, which is detrimental to the long term performance of the material.

The findings on the effect of biochar on the rutting susceptibility of the mix based on the flow number supported the dynamic modulus test result that the control mix seemed to be the most suitable mix for improving the rutting resistance of the asphalt mixture before and after long term ageing.

The effect of biochar on the fatigue cracking resistance of the mix and the moisture damage susceptibility of the mix are summarized below:

- The control mix had the highest fracture energy before moisture damage, which indirectly suggests that the control mix provides better resistance to fatigue cracking. This finding contradicts the result from the dynamic modulus test that the 10% slow pyrolysis biochar mix is better for fatigue cracking. From the variation in the results of the asphalt mixture properties evaluated based on the test procedures, it can be concluded that it is not enough to rely on one test method to determine the performance of asphalt mixtures.
- After moisture conditioning, the 10% slow pyrolysis biochar had the highest FI value, which suggests a better resistance to fatigue cracking. The higher the biochar content was, the better the mix seemed to perform in improving the cracking resistance of the mix.
- The 10% slow pyrolysis biochar seems to be the most preferred mix for improving the cracking resistance of the mix after moisture conditioning corresponds with the result from the dynamic modulus test.

From the study, it can be concluded that the slow pyrolysis biochar mix might be better at improving the thermal and fatigue cracking resistance of the asphalt mixture, while the use of biochar might be comprising the rutting resistance of the mix.

Factors that could have led to the variation in the test results obtained might be a human error during the mixing process of the biochar and the asphalt mix. The blending process was carried out by hand, and the rate of mixing would have been different for different mixes. The biochar particles could have settled at the bottom of the binder after it had been

in the oven for a while, so another quick mixing with a spatula was done before pouring it in the aggregate. The binder used for the control and 5% biochar mixes were from the same supply, while the binder used for the 10% biochar mix was supplied at a later date as the initial binder used was not sufficient. The difference in the supply might have affected the results as well. The different compaction efforts, varying sample sizes for the tests and different test procedures might have also contributed to the varying results. The asphalt mix was a dense mix based on the gradation of the aggregates.

The increase in the amount of filler used improves some properties of HMA mixtures while compromising other properties, as confirmed in this study. Typically, when the filler content is increased, the asphalt content needs to be reduced (Huang et al., 2007). However, the asphalt content was not reduced during the experiment when the filler content increased. This might have led to the mixtures with the 10% pyrolysis biochar outperforming the other mixtures in some of the asphalt mixture performance while compromising other performance attributes of the mix.

5.2.Recommendations

From the study, it is recommended that further testing be conducted. The asphalt mix design should be improved as the control mix was giving inconsistent results in the volumetric properties such as the air void content, BRD, and MRD after mixing and compaction. The mixing process of the biochar and the binder should be mechanically carried out with a shear blender or a mixer at the same rate and time for all the mixes. Also, biochar can be used as a modifier as opposed to a filler to determine what the impact will be on the mix. Other sources of biochar and different percentages of biochar by weight of

asphalt binder can be explored in future investigations. Also, the use of biochar should be considered in recycled mixtures or stone matrix asphalt (SMA).

The contribution of this study was a further investigation of the effect of biochar on the performance of dense graded asphalt mixtures.

6. REFERENCES

Al-Qadi, I.L., Ozer, H., Lambros, J., Khatib, A.E., Singhvi, P., Khan, T., Rivera-Perez, J., and Doll, B. 2015. Testing Protocols to Ensure Performance of High Asphalt Binder Replacement Mixes Using RAP and RAS.: 209.

American Association of State Highway and Transportation Officials (AASHTO) R 30-02. "Standard Practice for Mixture Conditioning of Hot Mix Asphalt (HMA)", Standard Specifications for Transportation Materials and Methods of Sampling and Testing, Part 1, 2020 Edition, Washington, D.C. (2019).

American Association of State Highway and Transportation Officials (AASHTO) R 62-13. "Standard Practice for Developing Dynamic Modulus Master Curves for Asphalt Mixtures", Standard Specifications for Transportation Materials and Methods of Sampling and Testing, Part 1, 2020 Edition, Washington, D.C. (2017).

American Association of State Highway and Transportation Officials (AASHTO) T 166-16. "Standard Specification for Bulk Specific Gravity (G_{mb}) of Compacted Asphalt Mixtures Using Saturated Surface-Dry Specimens", Standard Specifications for Transportation Materials and Methods of Sampling and Testing, Part 2, 2020 Edition, Washington, D.C. (2020).

American Association of State Highway and Transportation Officials (AASHTO) T 209-20. "Standard Method of Test for Theoretical Mximum Specific Gravity (G_{mm}) and Density of Asphalt Mixtures", Standard Specifications for Transportation Materials and Methods of Sampling and Testing, Part 2, 2020 Edition, Washington, D.C. (2020).

American Association of State Highway and Transportation Officials (AASHTO) T 269-14. "Standard Method of Test for Percent Air Voids in Compacted Dense and Open Asphalt Mixtures", Standard Specifications for Transportation Materials and Methods of Sampling and Testing, Part 2, 2020 Edition, Washington, D.C. (2018).

American Association of State Highway and Transportation Officials (AASHTO) T 283-14. "Standard Method of Test for Resistance of Compacted Asphalt Mixtures to Moisture-Induced Damage", Standard Specifications for Transportation Materials and Methods of Sampling and Testing, Part 2, 2020 Edition, Washington, D.C. (2018).

American Association of State Highway and Transportation Officials (AASHTO) T 312-19. "Standard Method of Test for Preparing and Determining the Density of Asphalt Mixture Specimens by Means of the Superpave Gyratory Compactor", Standard Specifications for Transportation Materials and Methods of Sampling and Testing, Part 2, 2020 Edition, Washington, D.C. (2019).

American Association of State Highway and Transportation Officials (AASHTO) T 342-11. "Standard Method of Test for Determining the Dynamic Modulus of Hot Mix Asphalt (HMA)", Standard Specifications for Transportation Materials and Methods of Sampling and Testing, Part 2, 2020 Edition, Washington, D.C. (2019).

American Association of State Highway and Transportation Officials (AASHTO) T 378-17. "Standard Method of Test for Determining the Dynamic Modulus and Flow Number for Asphalt Mixtures Using the Asphalt Mixture Performance Tester (AMPT)", Standard Specifications for Transportation Materials and Methods of Sampling and Testing, Part 2, 2020 Edition, Washington, D.C. (2017).

American Association of State Highway and Transportation Officials (AASHTO) TP 124-20. "Standard Method of Test for Determining the Fracture Potential of Asphalt Mixtures Using the Illinois Flexibility Index Test (I-FIT)", Standard Specifications for Transportation Materials and Methods of Sampling and Testing, Part 3, 2020 Edition, Washington, D.C. (2020).

Apeagyei, A.K. 2011. Correlating rutting with dynamic modulus of asphalt concrete. Proceedings of the Institution of Civil Engineers - Transport, 164(4): 241–249. ICE Publishing. doi:10.1680/tran.9.00056.

Asphalt Institute. 2007. The Asphalt Handbook. 7th ed. Lexington, Ky.: Asphalt Institute.

Asphalt Institute. 2014. MS-2 Asphalt Mix Design Methods. *In* 7th edition. Asphalt Institute, USA.

Asphaltmagazine.com. (2018). Applications for Asphalt Emulsions | Asphalt magazine. [online] Available at: http://asphaltmagazine.com/applications-for-asphalt-emulsions/.

Asphalt Paving Association of Iowa (APAI). 2005. Chapter 2 - Asphalt and Asphalt Paving Materials. *In* Asphalt Paving Association of Iowa., West Des Moines, IA.

Avanthi Deshani Igalavithana, Sanchita Mandal, Nabeel Khan Niazi, Meththika Vithanage, Sanjai J. Parikh, Fungai N. D. Mukome, Muhammad Rizwan, Patryk Oleszczuk, Mohammad Al-Wabel, Nanthi Bolan, Daniel C. W. Tsang, Ki-Hyun Kim & Yong Sik Ok. 2017. Advances and future directions of biochar characterization methods and applications, Critical Reviews in Environmental Science and Technology, 47:23, 2275-2330, DOI: 10.1080/10643389.2017.1421844.

Bardini, V.S. dos S., José, L.F.J., and Luis, M.G.K. 2013. INFLUENCE OF MINERAL FILLER ON VOLUMETRIC PROPERTIES OF HOT MIX ASPHALT. International Journal of Pavements Conference, São Paulo, Brazil, 156(1).

Basu, P. 2010. Biomass Gasification and Pyrolysis: Practical Design and Theory. *In* 1st edition. Academic Press.

Brown & Beattie Ltd. 2018. Retrieved from https://www.brownbeattie.com/site-finishes pavement/#iLightbox[092dc3c7679538944cf]/null.

Campbell, J., Sessions, J., Smith, D., and Trippe, K. 2018. Potential carbon storage in biochar made from logging residue: Basic principles and Southern Oregon case studies. Available from https://journals.plos.org/plosone/article?id=10.1371/journal.pone.0203475. [accessed 2 March 2020].

Carter, A., Donovan, H., MacInnis, K., Strynadka, T., and Association technique canadienne du bitume. 2018. Hot Mix Asphalt / Canadian technical Asphalt Association; Alan Carter, Hugh Donovan, Keith MacInnis and Todd Strynadka. *In* 1st edition. Canadian technical Asphalt Association.

CharGrow. 2018. Biochar vs. Charcoal vs. Activated Carbon: What They Are & How They Work. Available from https://char-grow.com/biochar-vs-charcoal-vs-activated-carbon. [accessed 18 May 2020].

Chebil S., Chaala A., and Roy C. 2002. Use of softwood bark charcoal as a modifier for road bitumen. Fuel 79(6), pp. 671-683.

Cheng, S., Chen, T., Xu, W., Huang, J., Jiang, S., & Yan, B. 2020. Application Research of Biochar for the Remediation of Soil Heavy Metals Contamination: A Review. Molecules (Basel, Switzerland), 25(14), 3167. https://doi.org/10.3390/molecules25143167

Dhyani aDhyani, V., and Bhaskar, T. (2019). "Chapter 9 - Pyrolysis of Biomass." Biofuels: Alternative Feedstocks and Conversion Processes for the Production of Liquid and Gaseous Biofuels (Second Edition), Biomass, Biofuels, Biochemicals, A. Pandey, C. Larroche, C.-G. Dussap, E. Gnansounou, S. K. Khanal, and S. Ricke, eds., Academic Press, 217–244.

The Globe and Mail. 2019. The high cost of Canada's 'free' roads. Available from https://www.theglobeandmail.com/opinion/editorials/article-the-high-cost-of-canadas-free-roads/. Globe editorial [accessed 10 December 2019].

Hersh, B., Mirkouei, A., Sessions, J., Rezaie, B., You, Y., Hersh, B., Mirkouei, A., Sessions, J., Rezaie, B., and You, Y. 2019. A review and future directions on enhancing sustainability benefits across food-energy-water systems: the potential role of biochar-derived products. AIMS Environmental Science, 6(5): 379–416. doi:10.3934/environsci.2019.5.379.

Huang, B., Shu, X., and Chen, X. 2007. Effects of mineral fillers on hot-mix asphalt laboratory-measured properties. International Journal of Pavement Engineering, 8: 1–9. doi:10.1080/10298430600819170.

Jeguirim, M., and Limousy, L. 2017. Biomass Chars: Elaboration, Characterization and Applications. Energies, 10(12): 2040. Multidisciplinary Digital Publishing Institute. doi:10.3390/en10122040.

King, G., King, H., Pavlovich, R., Epps, A., & Kandhal, P. (2018). Retrieved from http://www.amaac.org.mx/archivos/eventos/1cma_1999/31.pdf

Koul B., Taak P. 2018. Biochar and Soil Remediation. In: Biotechnological Strategies for Effective Remediation of Polluted Soils. Springer, Singapore. https://doi.org/10.1007/978-981-13-2420-8_5

Kumar, A., Choudhary, R., Narzari, R., Kataki, R., and Shukla, S.K. 2018. Evaluation of bio-asphalt binders modified with biochar: a pyrolysis by-product of Mesua ferrea seed cover waste. Cogent Engineering, 5(1): 1548534. doi:10.1080/23311916.2018.1548534.

Lee, Sze Ying & Sankaran, Revathy & Kit Wayne, Chew & Tan, Chung Hong & K, Rambabu & Show, Pau-Loke. 2019. Waste to bioenergy: a review on the recent conversion technologies. BMC Energy. 1. 10.1186/s42500-019-0004-7.

LTPP InfoPave - LTPPBind Online. 2021. Available from https://infopave.fhwa.dot.gov/Tools/LTPPBindOnline?mode=new. [accessed 2 February 2021].

MacInnis, K. 2018. Performance Graded Asphalt Cement | Hot Mix Asphalt. *In* 1st edition. Canadian Technical Asphalt Association.

Manyà, J.J. 2012. Pyrolysis for Biochar Purposes: A Review to Establish Current Knowledge Gaps and Research Needs. Environmental Science & Technology, 46(15): 7939–7954. doi:10.1021/es301029g.

McLaughlin, H. 2016. An Overview of the current Biochar and Activated Carbon Markets : Biofuels Digest. Available from https://www.biofuelsdigest.com/bdigest/2016/10/11/an-overview-of-the-current-biochar-and-activated-carbon-markets/. [accessed 18 May 2020].

National Academies of Sciences, Engineering, and Medicine. 2011. A Manual for Design of Hot-Mix Asphalt with Commentary. *In* www.nap.edu. The National Academies Press, Washington, DC.

National Academies of Sciences, Engineering, and Medicine. 2017. Relationship Between Chemical Makeup of Binders and Engineering Performance. Washington, DC: The National Academies Press. https://doi.org/10.17226/24850.

Pavement Interactive. 2018. Retrieved from https://www.pavementinteractive.org/reference-desk/materials/asphalt/asphalt-modifiers/

Rahbar-Rastegar, R., Dave, E.V., and Daniel, J.S. 2018. Fatigue and Thermal Cracking Analysis of Asphalt Mixtures Using Continuum-Damage and Cohesive-Zone Models. Journal of Transportation Engineering, Part B: Pavements, 144(4): 04018040. American Society of Civil Engineers. doi:10.1061/JPEODX.0000066.

Renaldo C. Walters, Elham H. Fini and Taher Abu-Lebdeh. 2014. Enhancing Asphalt Rheological Behavior and Aging Susceptibility Using Biochar and Nano-clay. American Journal of Engineering and Applied Sciences, Volume 7, Issue 1: pp. 66-76.

Roberts, F.L.; Kandhal, P.S.; Brown, E.R.; Lee, D.Y. and Kennedy, T.W. 1996. Hot Mix Asphalt Materials, Mixture Design, and Construction. National Asphalt Pavement Association Education Foundation. Lanham, MD.

Roy, N., Veeraragavan, A., and Murali Krishnan, J. 2015. Interpretation of flow number test data for asphalt mixtures. Proceedings of the Institution of Civil Engineers - Transport, 168(3): 191–199. doi:10.1680/tran.12.00070.

Sanchez, X., Somers, T., Dhasmana, H., Owolabi, O. (2020). *Effect of Biochar on the Basic Characteristics of Asphalt Mixtures*. Papagiannakis, A.T., Anupam, K., Bhasin, A., & Little, D. (Eds.). (2020). Advances in Materials and Pavement Performance Prediction II: Contributions to the 2nd International Conference on Advances in Materials and Pavement Performance Prediction (AM3P 2020), 27-29 May 2020, San Antonio, TX, USA (1st ed.). CRC Press. https://doi.org/10.1201/9781003027362

Shen, S., and Yu, H. 2011. Investigation of Dynamic Modulus and Flow Number Properties of Asphalt Mixtures in Washington State. (TNW2012-02).

Sivaprasad, S., Manandhar, A., and Shah, A. 2021. Hydrothermal Carbonization: Upgrading Waste Biomass to Char. Available from https://ohioline.osu.edu/factsheet/fabe-6622. [accessed 12 February 2021].

Souradeep Gupta and Harn Wei Kua. 2017. Factors Determining the Potential of Biochar as a Carbon Capturing and Sequestering Construction Material: Critical Review. Journal of Materials in Civil Engineering Vol. 29, Issue 9.

Spears, S. 2018. What is Biochar? Available from https://regenrationinternational.org/2018/05/16/what-is-biochar/.

Tan, Z., Lin, C.S.K., Ji, X., and Rainey, T.J. 2017. Returning biochar to fields: A review. Applied Soil Ecology, 116: 1–11. doi: 10.1016/j.apsoil.2017.03.017.

Townsend, E. 2016. Biochar – Gardening at Leisure. Available from https://www.gardeningatleisure.co.za/gardening/biochar/. [accessed 25 March 2020].

UG-GI-Glossary | Recycled Materials Resource Center. (n.d.). Available from https://rmrc.wisc.edu/ug-glossary/. [accessed 16 October 2020].

Varamini, S., Esenwa, M., Eng, P., and Tighe, S.L. 2017. Mixture Design and Field Experience: Coloured Hot Mix Asphalt on Bus Rapid Transit (BRT) Lanes in Ontario. Proceedings of the Sixth-Second Annual Conference of the Canadian Technical Asphalt Association (CTAA): Halifax, Nova Scotia, 89–103.

Virginia Asphalt Association. 2020. » Asphalt Binder/Cement. Available from https://vaasphalt.org/liquid-asphalt/. [accessed 20 January 2021].

Walker, D. (2018). The benefits of modified asphalts | Asphalt magazine. Retrieved from http://asphaltmagazine.com/the-benefits-of-modified-asphalts/.

Walters, R., Begum S.A., Fini E.H., and Abu-Lebdeh T.M. 2015. Investigating bio-char as flow modifier and water treatment agent for sustainable pavement design. American Journal of Engineering and Applied Sciences, v 8, n 1, 138-46, ISSN: 1941-7020.

Wani, I., Ramola, S., Garg, A., and Kushvaha, V. 2021. Critical review of biochar applications in geoengineering infrastructure: moving beyond agricultural and environmental perspectives. Biomass Conversion and Biorefinery. doi:10.1007/s13399-021-01346-8.

Wenhao, D., Feng, M., Chen, L., Zhen, F., Yue, H., and Jenny, L. 2020. Evaluation of Anti-Aging Performance of Biochar Modified Asphalt Binder. 10. doi:10.3390/coatings10111037.

Yu, H., Shen, D.S., Cooperation, I., Shen, S., and Yu, H. 2012. An Investigation of Dynamic Modulus and Flow Number Properties of Asphalt Mixtures in Washington State.

Zama, Eric & Reid, Brian & Arp, Hans Peter & Sun, Guo-Xin & Yuan, Haiyan. (2018). Advances in research on the use of biochar in soil for remediation: a review. Journal of Soils and Sediments. 18. 1-18. 10.1007/s11368-018-2000-9.

Zhao S., Huang B., Shu X., and Ye P. 2014. Laboratory Investigation of Biochar-Modified Asphalt Mixture. Transportation Research Record, vol. 2445, 1: pp. 56-63.

Zhao S., Huang B., Ye X.P., Shu X., and Jia X. 2014. Utilizing bio-char as a bio-modifier for asphalt cement: A sustainable application of bio-fuel by-product. Fuel 133, pp. 52-62.

Zhou, X., Adhikari, S. 2019. Flow-induced crystallization of biochar in bio-asphalt under various aging conditions. Science of the Total Environment 695,133943

Appendix A. Asphalt Mix Design & LTPPBind Data

GEMTEC
Consulting Engineers and Scientists

Asphalt Concrete Mix Design
Superpave

Client: [redacted]
Project: [redacted]
Project#: [redacted] Date Completed: July 10, 2019

Mix Type	D	Material	BRD	Lottman Properties		RAP Properties		Superpave Properties	
Design Gyrations	75	12.5-6.3 mm	2.727					N7	85.5
AC Type	MeAsphalt 58S-28	6.3-0 mm	2.679	TSR (virgin)	--	BRD (coarse)	NA	N75	95.7
Mixing Temp	125-130 C	6.3-0 mm Washed	2.682	Antistrip Rqd	Yes	BRD (fine)	NA	N115	97.9
AC Relative Density	1.020	Colter Blend Sand	2.568	Additive	Evotherm	AC Content	NA	Dry Briquette Wt	4494.5 g
Compaction Temp	120 C			Dosage	0.30%			Mix Briquette Wt (selected)	4781.4 g
Mix AC Content (Virgin)	6.00%	Combined BRD	2.688	TSR (additive)	--			Height at N100	115.0 mm
WMA Technology	Evotherm								

Aggregate Source	Aggregate Type	Aggregate Percent	Percent Passing											
			25 000	19 000	16 000	12 500	9 500	6 300	4 750	2 360	1 180	600	300	150	75
SIL Q2	12.5-6.3 mm	37	100.0	100.0	100.0	100.0	78.0	21.0	6.5	2.5	1.8	1.4	1.3	1.2	1.1
SIL Q2	6.3-0 mm	41	100.0	100.0	100.0	100.0	100.0	98.4	88.5	50.3	30.0	19.5	13.4	10.1	8.7
SIL Q1	6.3-0 mm Washed	14	100.0	100.0	100.0	100.0	100.0	97.8	86.5	50.4	29.1	17.3	10.6	6.9	5.1
Colter	Colter Blend Sand	8	100.0	100.0	100.0	100.0	100.0	100.0	99.7	99.2	98.1	92.2	63.4	23.1	9.2
Combined Gradation			100.0	100.0	100.0	100.0	91.9	69.8	58.8	36.5	24.9	18.3	12.5	7.4	5.4
Specification						100	76-98	60-84	52-70	36-65	20-55	16-44	8-26	4-12	2-6

Trial	AC %	MTRD	BRD	Air Voids %	VMA %	VFA %	Film Thickness microns	Effective AC %	Absorbed AC %	Dust/ Binder Ratio
1	5.00	2.543	2.344	7.8	17.2	54.4	7.8	4.06	0.99	1.336
2	5.50	2.522	2.369	6.1	16.7	63.7	8.9	4.58	0.97	1.184
3	6.00	2.501	2.394	4.3	16.3	73.7	10.0	5.11	0.94	1.061
4	6.50	2.480	2.419	2.5	15.9	84.5	11.1	5.65	0.91	0.960
5	7.00	2.459	2.444	0.6	15.4	96.0	12.2	6.19	0.87	0.876
Selected	**6.00**	**2.501**	**2.394**	**4.3**	**16.3**	**73.7**	**10.0**	**5.11**	**0.94**	**1.061**
Specification				3.0-5.0	15.5-17	70-77	>8.5			0.6-1.2

Figure A. 1: Type D NBDTI Mix Design Provided by GEMTEC Consulting

General Project Information

Project Number: 1
Project Title: Flow number test
Project Description: Obtaining the adjusted PG temperature for a flow number test.

Climatic Data Source (MERRA)

Latitude, Degree: 45.96359
Longitude, Degree: -66.64312

Climatic Data

Lowest Yearly Air Temperature, ºC: -29.85
Low Air Temp Standard Deviation, ºC: 4.23
Yearly Degree-Days > 10 Deg. ºC: 1641.63
High Air Temperature of high 7 days: 27.23
Standard Dev. of the high 7 days: 1.24
Low Pavement Temperature 50%: -31.20
Low Pavement Temperature 98%: -38.80
High Avg Pavement Temperature of 7 Days 50%: 49.36
High Avg Pavement Temperature of 7 Days 98%: 53.11

Target Rut Depth

Target Rut Depth (mm): 12.5

Temperature Adjustments

Depth of Layer, mm: 20
Base HT PG: 52

Traffic Adjustments

Traffic loading Cumulative ESAL for the Design Period, Millions: 10
Traffic Speed (Fast: >70 km/h, Slow: 20-70 km/h, Standing: < 20 km/h): Slow

Performance Grade

AASHTO M323-13 Performance-Graded Asphalt Binder		
PG Temperature	**High**	**Low**
Performance Grade Temperature at 50% Reliability	43.6	-22.8
Performance Grade Temperature at 98% Reliability	46.4	-30.4
Adjustment for Traffic (AASHTO M323-13)	15.5	
Adjustment for Depth	-3.9	1.6
Adjusted Performance Grade Temperature	58.0	-28.8
Selected PG Grade	**58**	**-34**
PG Grade	**M323, PG 58-34**	

Figure A. 2: High Adjusted PG Temperature Obtained from LTPPBind

Appendix B. Dynamic Modulus Test Data and Master Curves

Table B. 1: Dynamic Modulus Test Data for the Short Term Aged Control Mix

Temp, °C	Freq, Hz	E*, MPa	CV, %	Phase angle, degree	Std Dev. phase angle
-10.0	25	18220.4	31.6	7.6	0.3
-10.0	10	16967.4	29.5	8.1	0.4
-10.0	5	16067.8	28.6	8.7	0.3
-10.0	1	13893.5	29.4	10.0	0.8
-10.0	0.5	12960.4	28.8	10.8	0.9
-10.0	0.1	10796.4	28.2	13.0	1.2
4.4	25	11110.4	21.1	13.8	1.1
4.4	10	10122.9	17.6	15.0	0.9
4.4	5	9204.6	16.7	16.1	1.0
4.4	1	6799.8	18.7	19.8	1.3
4.4	0.5	5918.9	18.8	21.5	1.5
4.4	0.1	4001.9	20.8	25.9	1.9
21.1	25	5032.3	12.6	25.1	1.3
21.1	10	3932.0	13.7	26.5	1.2
21.1	5	3158.8	15.7	28.0	1.3
21.1	1	1735.3	20.7	31.5	0.9
21.1	0.5	1339.5	22.5	31.8	0.5
21.1	0.1	698.2	25.7	31.8	0.4
37.8	25	1422.6	14.0	33.1	0.3
37.8	10	961.4	15.8	32.6	0.4
37.8	5	711.7	16.8	32.2	0.6
37.8	1	338.5	19.9	31.1	0.9
37.8	0.5	263.5	20.3	29.2	1.1
37.8	0.1	157.7	21.6	25.0	2.0

Table B. 2: Dynamic Modulus Test Data for the Long Term Aged Control Mix

Temp, °C	Freq, Hz	E*, MPa	CV, %	Phase angle, degree	Std Dev. phase angle
-10.0	25	18925.4	34.4	6.7	0.6
-10.0	10	18055.3	32.9	7.0	0.5
-10.0	5	17345.2	31.8	7.3	0.4
-10.0	1	15242.4	31.7	8.6	0.6
-10.0	0.5	14409.4	31.2	9.2	0.6
-10.0	0.1	12436.4	30.7	10.8	0.5
4.4	25	12213.9	16.2	11.9	0.3
4.4	10	11214.1	14.6	13.0	0.6
4.4	5	10297.6	14.7	14.0	0.7
4.4	1	7964.1	15.8	17.2	1.0
4.4	0.5	7073.1	16.2	18.8	1.1
4.4	0.1	5080.8	18.3	23.1	1.4
21.1	25	6196.3	16.7	22.8	0.9
21.1	10	4960.6	16.7	24.5	1.1
21.1	5	4109.8	17.7	26.3	1.0
21.1	1	2386.8	21.0	30.7	1.2
21.1	0.5	1894.2	23.0	31.7	1.3
21.1	0.1	1006.0	26.4	33.2	1.4
37.8	25	1942.0	34.3	32.8	2.2
37.8	10	1311.1	37.9	33.5	1.7
37.8	5	958.4	40.5	33.7	1.3
37.8	1	448.4	44.5	34.0	1.0
37.8	0.5	334.5	44.7	32.4	1.0
37.8	0.1	184.5	42.2	27.7	1.8

Table B. 3: Dynamic Modulus (Short Term Aged 5% Slow Pyrolysis Biochar Mix)

Temp, °C	Freq, Hz	E*, MPa	CV, %	Phase angle, degree	Std Dev. phase angle
-10.0	25	13562.9	30.1	7.7	1.6
-10.0	10	12593.6	26.7	7.9	1.2
-10.0	5	12005.6	24.6	8.2	0.9
-10.0	1	10488.9	25.0	9.4	0.7
-10.0	0.5	9834.5	23.3	10.1	0.8
-10.0	0.1	8268.6	19.7	12.2	0.9
4.4	25	9099.7	12.1	13.6	0.7
4.4	10	8350.2	6.7	14.9	1.0
4.4	5	7621.4	5.3	16.0	1.1
4.4	1	5657.4	4.8	19.9	1.3
4.4	0.5	4945.1	3.8	21.8	1.4
4.4	0.1	3312.5	3.5	26.9	1.8
21.1	25	4494.0	7.3	26.0	0.9
21.1	10	3410.9	9.3	28.0	1.1
21.1	5	2673.1	11.1	29.9	1.2
21.1	1	1369.3	16.3	33.5	1.2
21.1	0.5	1014.8	18.3	34.0	1.2
21.1	0.1	491.9	21.1	34.1	1.3
37.8	25	1147.0	18.3	35.3	1.2
37.8	10	729.2	21.3	35.2	1.1
37.8	5	502.7	23.5	35.0	1.6
37.8	1	222.2	28.6	33.6	1.7
37.8	0.5	167.1	29.0	31.4	1.4
37.8	0.1	98.3	28.9	25.5	0.8

Table B. 4: Dynamic Modulus (Long Term Aged 5% Slow Pyrolysis Biochar Mix)

Temp, °C	Freq, Hz	E*, MPa	CV, %	Phase angle, degree	Std Dev. phase angle
-10.0	25	19021.6	22.0	5.8	0.3
-10.0	10	17919.8	21.2	6.5	0.2
-10.0	5	17075.3	20.6	6.9	0.1
-10.0	1	15054.2	20.8	8.1	0.2
-10.0	0.5	14192.7	20.6	8.8	0.2
-10.0	0.1	12135.5	20.4	10.6	0.3
4.4	25	12727.6	19.3	11.3	0.3
4.4	10	11228.5	17.3	12.6	0.4
4.4	5	10203.0	16.9	13.7	0.4
4.4	1	7853.8	16.9	17.2	0.5
4.4	0.5	6914.7	16.3	18.8	0.6
4.4	0.1	4884.7	15.2	23.1	0.7
21.1	25	5821.9	11.7	22.1	0.8
21.1	10	4694.9	10.3	24.0	0.9
21.1	5	3893.8	10.1	25.7	0.9
21.1	1	2279.0	9.8	30.2	1.2
21.1	0.5	1791.0	9.8	31.3	1.3
21.1	0.1	948.3	9.6	33.2	1.5
37.8	25	1727.3	9.0	33.1	1.3
37.8	10	1161.5	11.7	33.9	1.7
37.8	5	842.5	13.8	34.2	1.8
37.8	1	390.2	17.5	34.5	1.9
37.8	0.5	291.2	17.9	33.1	2.0
37.8	0.1	160.4	13.9	29.0	2.3

Table B. 5: Dynamic Modulus (Short Term Aged 5% Fast Pyrolysis Biochar Mix)

Temp, °C	Freq, Hz	E*, MPa	CV, %	Phase angle, degree	Std Dev. phase angle
-10.0	25	18642.9	19.0	7.8	1.0
-10.0	10	17376.4	18.2	8.3	0.7
-10.0	5	16386.5	17.7	8.9	0.7
-10.0	1	14021.8	18.1	10.6	1.0
-10.0	0.5	13011.6	17.9	11.5	1.0
-10.0	0.1	10642.4	18.3	14.2	1.0
4.4	25	10725.7	9.6	14.7	0.3
4.4	10	9362.3	9.7	16.2	0.5
4.4	5	8312.1	10.3	17.7	0.5
4.4	1	5966.4	12.0	22.3	0.9
4.4	0.5	5065.2	13.4	24.5	1.1
4.4	0.1	3183.6	17.2	30.1	1.5
21.1	25	4542.1	21.2	27.3	2.3
21.1	10	3395.0	24.2	29.5	2.5
21.1	5	2662.5	27.6	31.4	2.5
21.1	1	1359.6	33.5	35.2	2.5
21.1	0.5	1020.9	37.0	35.6	2.7
21.1	0.1	484.1	39.2	35.5	3.1
37.8	25	1148.0	28.8	36.2	1.8
37.8	10	742.5	32.3	35.8	2.0
37.8	5	532.3	34.9	35.2	2.3
37.8	1	249.9	38.9	33.0	1.6
37.8	0.5	192.7	39.2	30.5	1.1
37.8	0.1	119.9	37.5	24.1	0.9

Table B. 6: Dynamic Modulus (Long Term Aged 5% Fast Pyrolysis Biochar Mix)

Temp, °C	Freq, Hz	E*, MPa	CV, %	Phase angle, degree	Std Dev. phase angle
-10.0	25	20977.3	22.0	5.7	0.9
-10.0	10	19786.9	22.5	6.2	0.7
-10.0	5	18868.8	23.2	6.7	0.7
-10.0	1	16677.7	25.3	8.0	0.8
-10.0	0.5	15733.9	26.1	8.6	0.8
-10.0	0.1	13502.7	28.0	10.3	0.9
4.4	25	12363.9	17.1	11.9	0.5
4.4	10	10928.3	13.9	13.1	0.6
4.4	5	9906.1	12.2	14.3	0.7
4.4	1	7591.3	12.6	17.8	0.8
4.4	0.5	6671.6	11.7	19.6	0.8
4.4	0.1	4706.8	10.7	24.0	0.8
21.1	25	5801.2	8.9	22.3	0.3
21.1	10	4666.0	7.5	24.1	0.3
21.1	5	3839.0	7.6	25.7	0.3
21.1	1	2238.8	7.9	30.2	0.3
21.1	0.5	1752.4	7.9	31.4	0.5
21.1	0.1	918.0	7.8	33.2	1.1
37.8	25	1776.6	8.6	33.2	1.6
37.8	10	1169.1	11.2	34.1	1.4
37.8	5	844.6	13.2	34.2	1.6
37.8	1	378.5	16.2	34.7	1.8
37.8	0.5	278.7	16.7	33.3	1.5
37.8	0.1	148.0	14.7	28.9	0.5

Table B. 7: Dynamic Modulus (Short Term Aged 10% Slow Pyrolysis Biochar Mix)

Temp, °C	Freq, Hz	E*, MPa	CV, %	Phase angle, degree	Std Dev. phase angle
-10.0	25	16614.6	8.5	7.6	0.2
-10.0	10	15316.7	8.3	8.1	0.2
-10.0	5	14449.2	8.3	8.7	0.2
-10.0	1	12351.8	8.1	10.5	0.3
-10.0	0.5	11441.4	8.0	11.5	0.3
-10.0	0.1	9292.0	7.8	14.4	0.5
4.4	25	9325.5	10.6	14.7	0.1
4.4	10	8032.1	10.1	16.3	0.1
4.4	5	7114.0	9.7	17.9	0.2
4.4	1	5017.2	9.0	22.7	0.3
4.4	0.5	4228.4	8.7	24.9	0.3
4.4	0.1	2629.5	7.9	30.2	0.3
21.1	25	3468.1	8.9	28.9	0.2
21.1	10	2575.1	8.1	30.7	0.4
21.1	5	1959.2	7.0	32.5	0.5
21.1	1	964.2	6.5	35.5	0.8
21.1	0.5	709.5	7.0	35.4	1.1
21.1	0.1	337.6	7.6	35.0	1.3
37.8	25	878.3	18.2	36.9	1.3
37.8	10	554.6	19.2	36.0	0.8
37.8	5	379.6	20.6	35.7	1.0
37.8	1	168.7	21.5	33.6	1.2
37.8	0.5	132.5	22.3	30.3	1.4
37.8	0.1	79.4	11.0	24.4	1.2

Table B. 8: Dynamic Modulus (Long term Aged 10% Slow Pyrolysis Biochar Mix)

Temp, °C	Freq, Hz	E*, MPa	CV, %	Phase angle, degree	Std Dev. phase angle
-10.0	25	16098.0	15.1	6.9	0.3
-10.0	10	15021.2	14.6	7.3	0.4
-10.0	5	14268.3	14.4	7.8	0.4
-10.0	1	12467.5	14.7	9.0	0.3
-10.0	0.5	11677.5	14.6	9.6	0.3
-10.0	0.1	9807.9	14.3	11.7	0.4
4.4	25	9970.9	13.6	12.6	0.9
4.4	10	8844.5	11.7	14.0	0.8
4.4	5	8004.5	11.5	15.1	0.9
4.4	1	6030.5	12.8	18.7	1.0
4.4	0.5	5272.5	13.0	20.5	1.1
4.4	0.1	3647.7	14.2	25.0	1.2
21.1	25	4572.9	6.3	24.0	0.8
21.1	10	3606.6	7.1	25.6	0.8
21.1	5	2915.3	8.4	27.2	0.8
21.1	1	1640.9	12.0	31.2	0.5
21.1	0.5	1266.5	13.5	31.9	0.5
21.1	0.1	657.1	15.6	33.1	0.5
37.8	25	1379.7	25.1	33.9	2.1
37.8	10	921.1	27.5	34.1	1.7
37.8	5	673.7	29.2	33.7	1.5
37.8	1	318.4	29.3	33.1	1.2
37.8	0.5	242.0	27.2	31.3	1.5
37.8	0.1	136.0	18.2	26.6	2.3

Table B. 9: Dynamic Modulus (Short Term Aged 10% Fast Pyrolysis Biochar Mix)

Temp, °C	Freq, Hz	E*, MPa	CV, %	Phase angle, degree	Std Dev. phase angle
-10.0	25	14369.9	17.5	7.3	0.1
-10.0	10	13492.4	17.9	8.0	0.1
-10.0	5	12766.0	17.7	8.6	0.1
-10.0	1	10881.8	16.8	10.2	0.1
-10.0	0.5	10112.0	16.8	11.1	0.2
-10.0	0.1	8273.8	16.6	13.7	0.3
4.4	25	9576.0	18.5	13.9	0.4
4.4	10	8443.8	16.4	15.5	0.1
4.4	5	7559.8	15.8	16.9	0.1
4.4	1	5458.1	16.0	21.2	0.4
4.4	0.5	4670.8	15.8	23.2	0.5
4.4	0.1	3001.9	17.3	28.5	1.0
21.1	25	3765.0	18.5	28.2	1.5
21.1	10	2836.1	19.6	30.0	1.2
21.1	5	2219.8	21.8	31.7	1.1
21.1	1	1124.9	27.1	35.1	0.8
21.1	0.5	837.5	28.0	35.3	0.8
21.1	0.1	410.0	28.1	34.7	1.4
37.8	25	959.2	7.9	37.5	1.2
37.8	10	604.9	9.5	37.1	1.5
37.8	5	419.1	10.2	36.9	2.0
37.8	1	187.3	11.8	34.8	2.8
37.8	0.5	144.7	15.4	32.0	3.9
37.8	0.1	96.1	21.2	24.9	3.2

Table B. 10: Dynamic Modulus (Long Term Aged 10% Fast Pyrolysis Biochar Mix)

Temp, °C	Freq, Hz	E*, MPa	CV, %	Phase angle, degree	Std Dev. phase angle
-10.0	25	16458.8	17.5	6.8	0.5
-10.0	10	15169.7	15.8	7.4	0.6
-10.0	5	14359.1	15.6	7.8	0.6
-10.0	1	12484.6	15.6	9.2	0.6
-10.0	0.5	11682.6	15.4	9.9	0.6
-10.0	0.1	9772.2	14.9	12.0	0.7
4.4	25	10600.3	8.4	13.0	0.7
4.4	10	9335.6	6.7	14.0	0.6
4.4	5	8439.4	6.3	15.2	0.6
4.4	1	6370.7	5.7	18.7	0.7
4.4	0.5	5585.2	5.5	20.4	0.8
4.4	0.1	3884.2	5.1	24.6	0.9
21.1	25	4595.5	1.9	23.9	0.6
21.1	10	3621.4	1.6	25.7	0.4
21.1	5	2946.4	2.8	27.3	0.4
21.1	1	1658.7	5.2	31.5	0.2
21.1	0.5	1283.4	6.6	32.4	0.2
21.1	0.1	662.8	7.8	33.8	0.2
37.8	25	1391.8	15.4	33.4	0.7
37.8	10	924.0	17.5	34.0	0.6
37.8	5	667.1	19.1	34.1	0.6
37.8	1	300.4	20.3	34.3	0.6
37.8	0.5	223.0	19.5	32.7	1.0
37.8	0.1	120.3	12.9	28.4	1.7

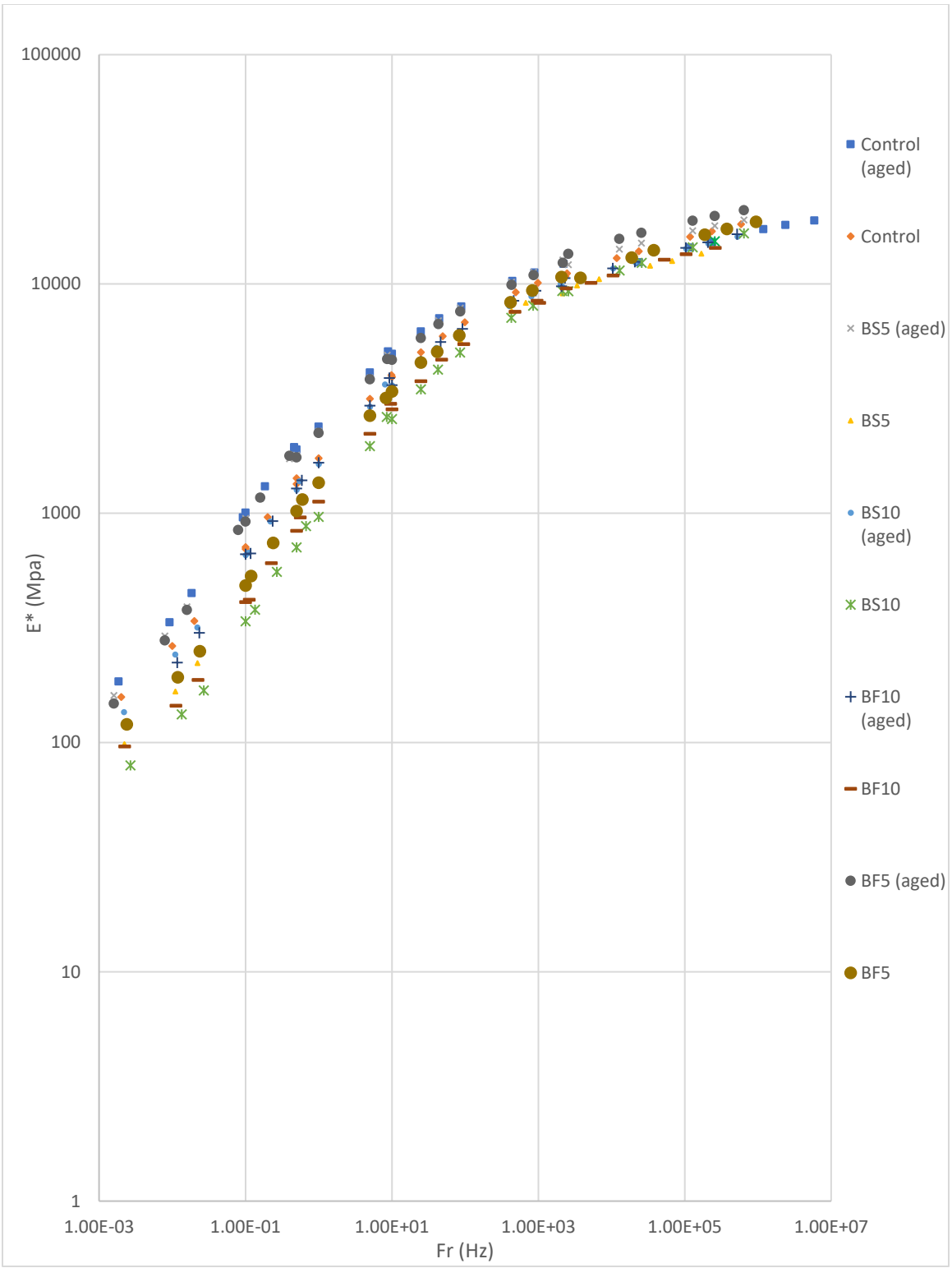

Figure B. 1: Composite Master Curve (Before and After Conditioning)

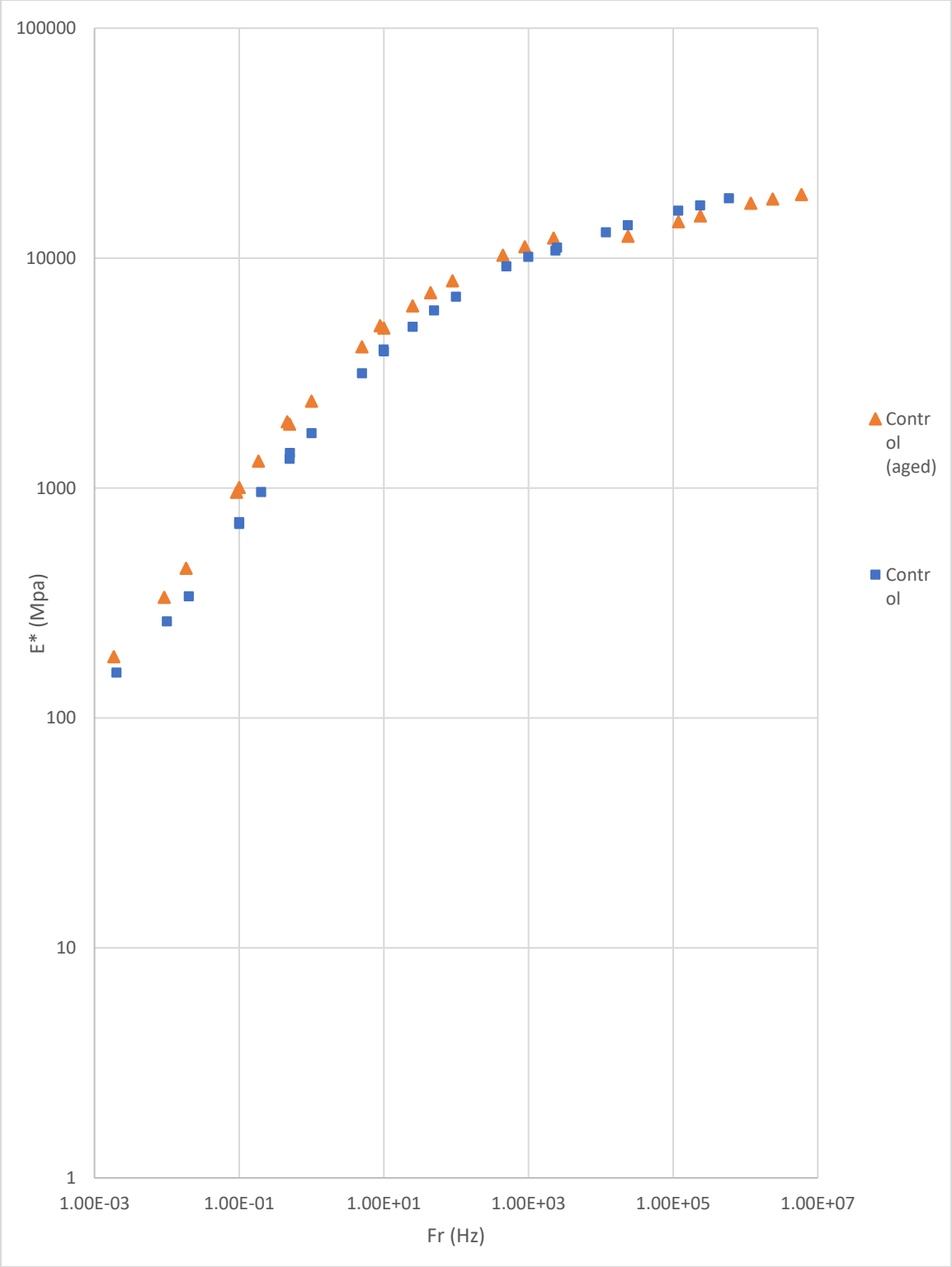

Figure B. 2: Master Curve of Short Term Aged vs Long Term Aged Control Mix

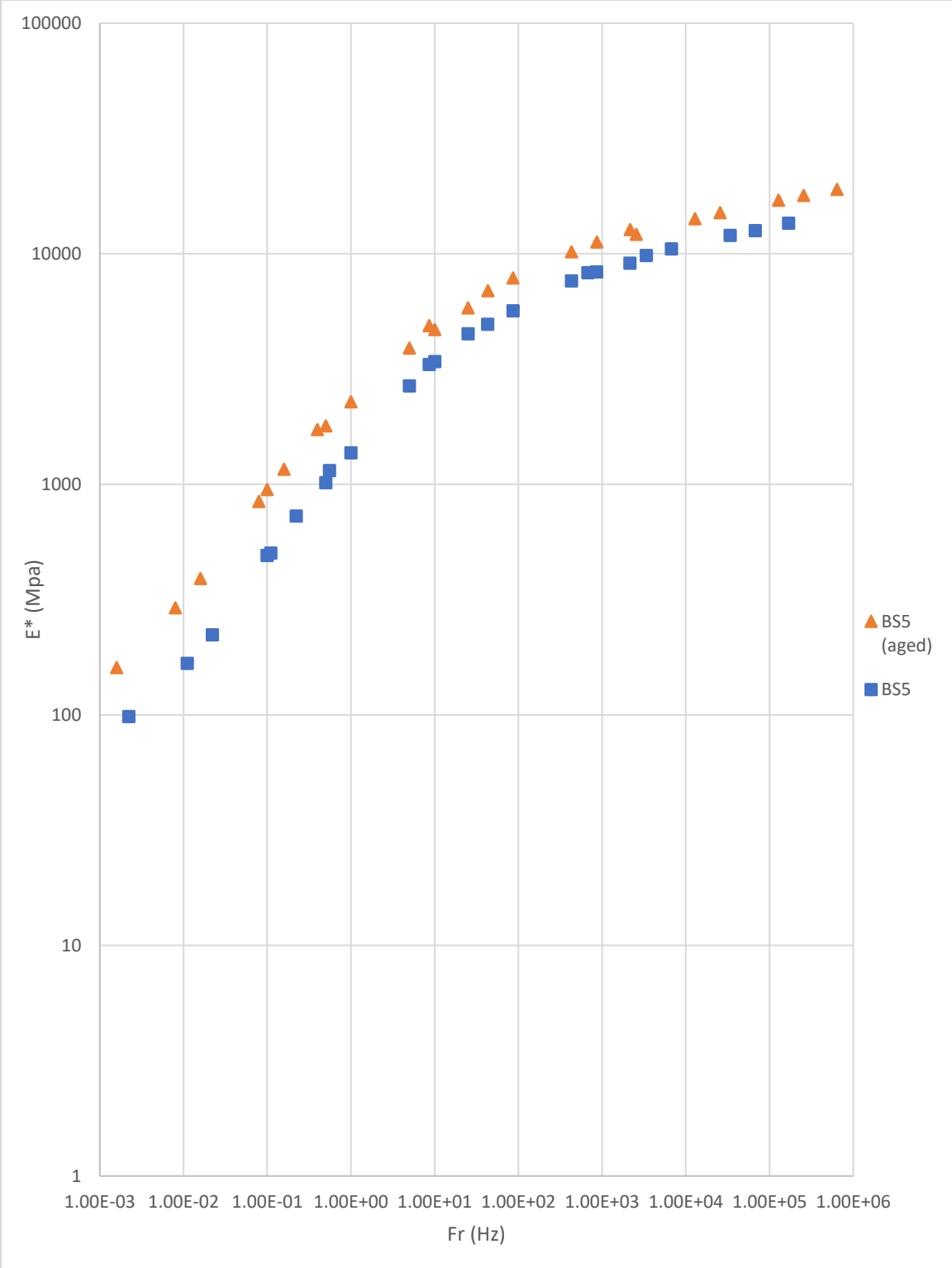

Figure B. 3: Master Curve (Short vs Long term Aged 5% Slow Pyrolysis Biochar)

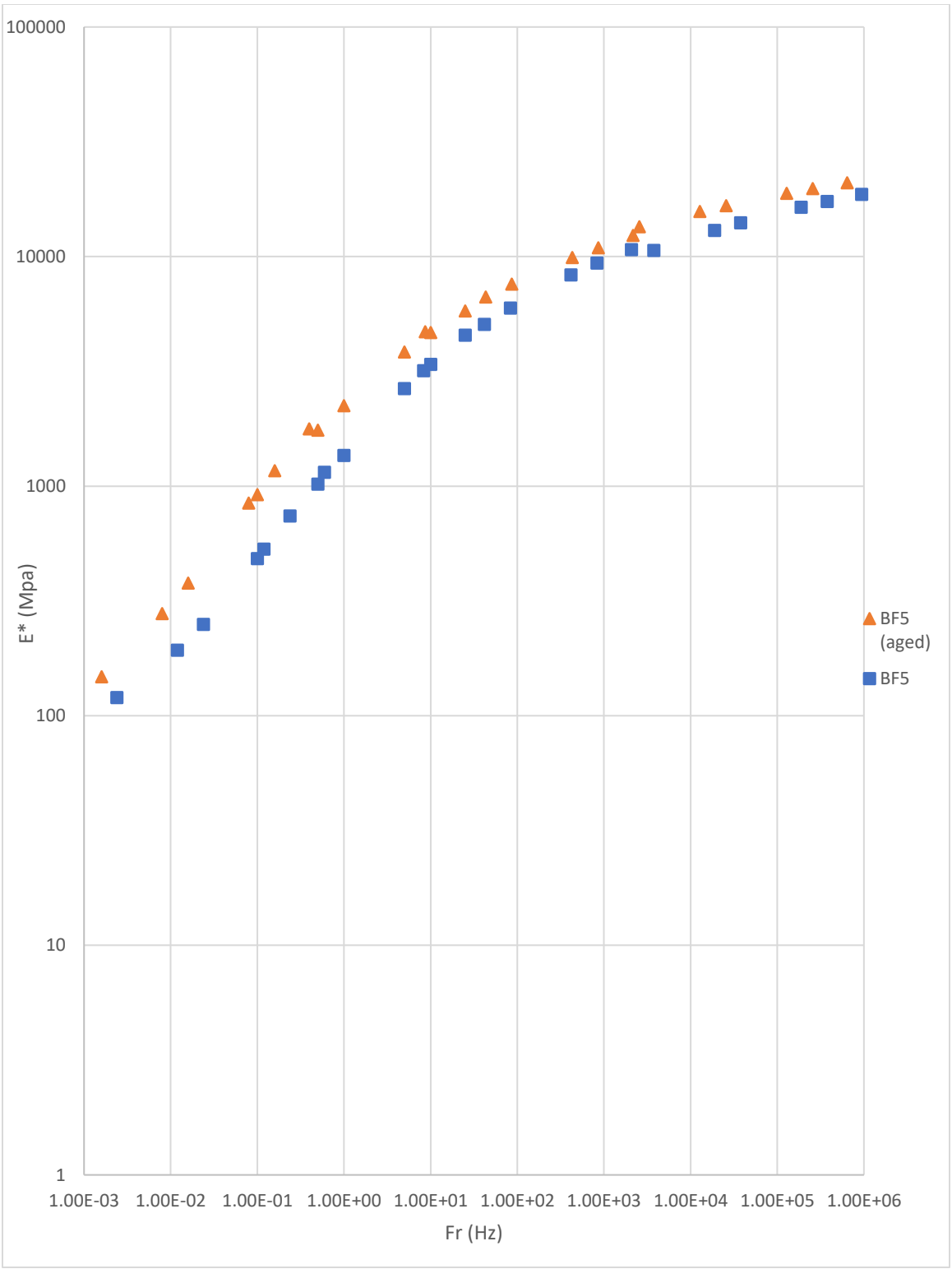

Figure B. 4: Master Curve (Short vs Long Term Aged 5% Fast Pyrolysis Biochar)

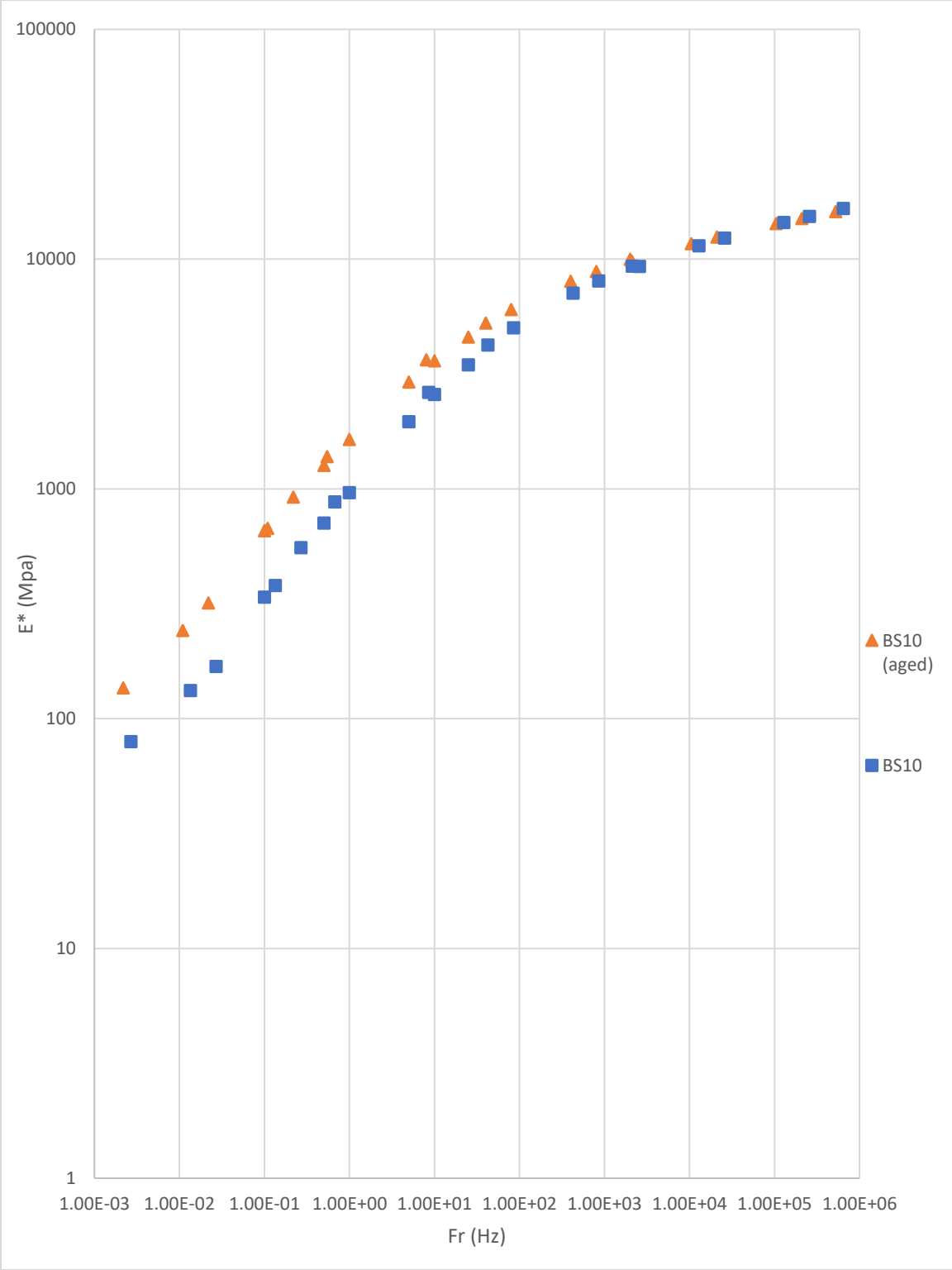

Figure B. 5: Master Curve (Short vs Long Term Aged 10% Slow Pyrolysis Biochar)

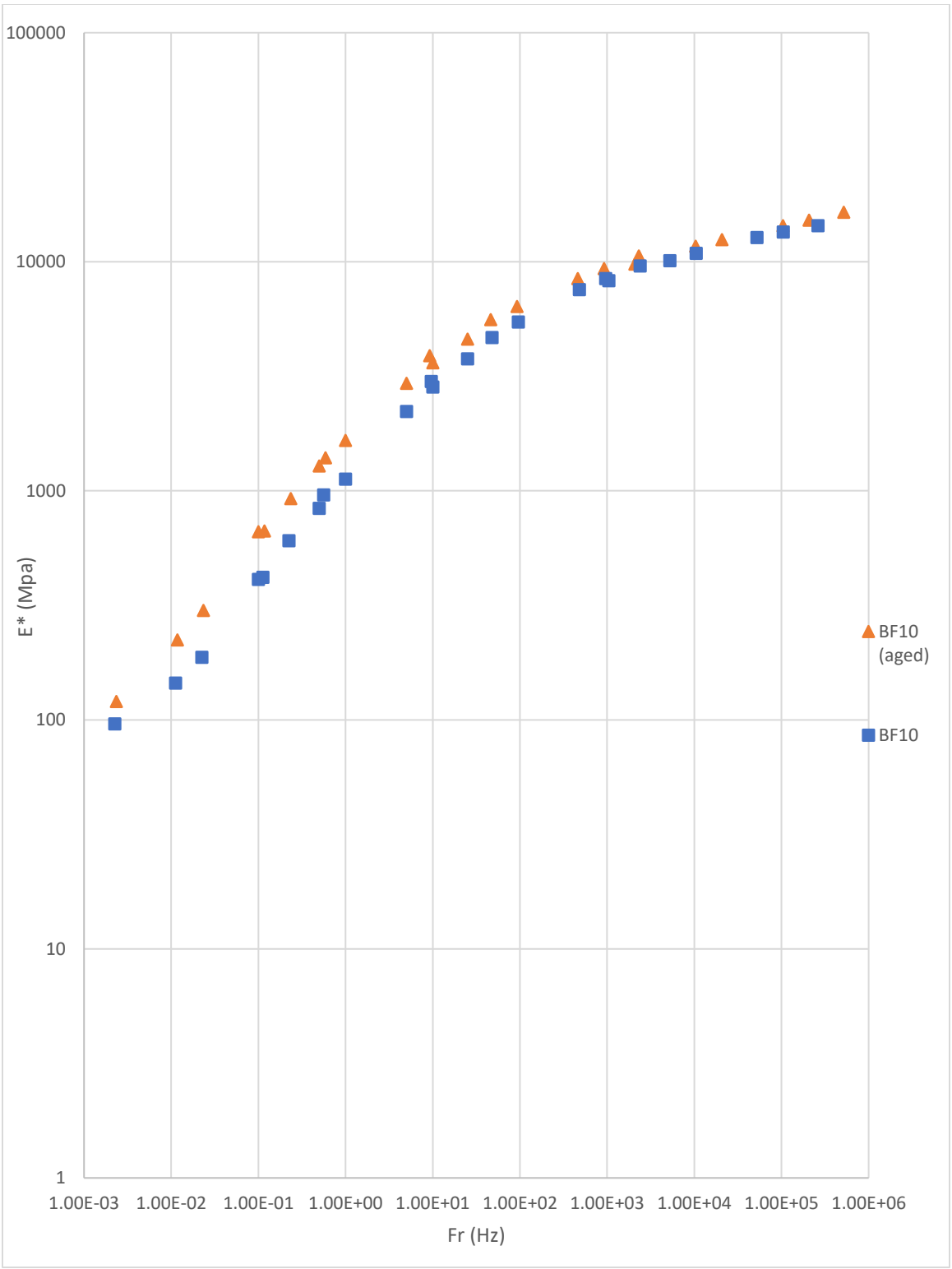

Figure B. 6: Master Curve (Short vs Long Term Aged 10% Fast Pyrolysis Biochar)

Table B. 11: Fitting Parameters (Master Curve of the Short Term Aged Mixes)

Mix	δ	α	β	γ	a-10	a4	a21	a37
Control	1.4572	2.8204	-0.5453	0.5803	4.3728	1.9953	0	-1.6981
BS5	1.2948	2.8390	-0.6277	0.6709	3.8293	1.9351	0	-1.6547
BF5	1.4901	2.7621	-0.3840	0.6438	4.5766	1.9203	0	-1.6220
BS10	1.1250	3.1163	-0.4070	0.6065	4.4117	1.9309	0	-1.5697
BF10	1.3280	2.8441	-0.4415	0.6494	4.0205	1.9825	0	-1.6482

Table B. 12: Fitting Parameters (Master Curve of the Long term Aged Mixes)

Mix	δ	α	β	γ	a-10	a4	a21	a37
Control	1.5002	2.7412	-0.7883	0.6198	5.3750	1.9483	0	-1.7338
BS5	1.4066	2.8783	-0.7434	0.5922	4.4093	1.9365	0	-1.7980
BF5	1.4066	2.8783	-0.7434	0.5922	4.4093	1.9365	0	-1.7980
BS10	1.2718	2.9498	-0.6624	0.5794	4.3216	1.9042	0	-1.6599
BF10	1.3011	2.9145	-0.6476	0.6144	4.3173	1.9653	0	-1.6292

Appendix C. Flow Number Test Data

Table C. 1: Flow Number Test Data for the Short Term Aged Samples

Mix type	Sample	Flow Number	Average	Standard deviation
Control	CL1	36	30.7	5.0
	CL3	30		
	CL5	26		
BS5	BS52	14	20.7	5.9
	BS53	25		
	BS54	23		
BF5	BF51	15	14.7	0.6
	BF52	14		
	BF53	15		
BS10	BS101	9	10	1.0
	BS102	10		
	BS104	11		
BF10	BF102	13	13.0	0.0
	BF103	13		
	BF106	13		

Table C. 2: Flow Number Test Data for the Long Term Aged Samples

Mix type	Sample	Flow Number	Average	Standard deviation
Control	CL2	32	36.3	8.4
	CL4	46		
	CL6	31		
BS5	BS55	23	26.7	3.5
	BS56	27		
	BS58	30		
BF5	BF54	49	58.0	9.0
	BF55	67		
	BF56	58		
BS10	BS103	14	17.3	3.1
	BS106	18		
	BS107	20		
BF10	BF101	23	22.0	3.6
	BF105	18		
	BF107	25		

Appendix D. Fracture Energy and Flexibility Index Test Data

Table D. 1: Flexibility Index Test Data for the Unconditioned Specimens

Mix type	Sample	W_f (J)	m (kN/mm)	L_{lig} (mm)	t_{lig} (mm)	A_{lig} (mm)	G_f (J/m^2)	FI	Avg GF	Avg FI
Control	CS1B	11.6	-0.7	60.25	56.00	3373.80	3438.26	49.12	2967.04	44.36
	CS2B	9.0	-0.7	59.89	50.48	3023.22	2976.96	42.52		
	CS4B	8.2	-0.6	59.62	55.33	3928.59	2485.91	41.43		
BS5	BS52A	6.1	-1.1	58.77	50.40	2961.74	2059.60	18.72	2038.49	20.68
	BS52B	6.9	-0.8	59.61	50.70	3021.95	2283.29	28.54		
	BS53A	5.0	-1.2	55.05	51.24	2820.75	1772.58	14.77		
BF5	BF51B	8.3	-0.8	62.55	50.78	3176.16	2613.22	32.67	2631.62	29.50
	BF52A	7.9	-1.0	61.33	50.26	3082.01	2563.26	25.63		
	BF52B	7.9	-0.9	58.38	49.78	2906.14	2718.39	30.20		
BS10	BS101B	4.8	-0.5	55.22	51.21	2827.94	1697.35	33.95	2026.15	35.79
	BS104B	6.9	-0.5	54.64	50.79	2775.17	2486.34	49.73		
	BS105B	6.0	-0.8	62.32	50.81	3166.61	1894.77	23.69		
BF10	BF102A	4.2	-0.4	55.62	49.53	2754.85	1524.60	38.10	1565.50	39.15
	BF103A	5.0	-0.4	63.20	49.25	3112.60	1606.40	40.20		

Table D. 2: Flexibility Index Test Data for the Moisture Conditioned Specimens

Mix type	Sample	W_f (J)	m (kN/mm)	L_{lig} (mm)	t_{lig} (mm)	A_{lig} (mm)	G_f (J/m^2)	FI	Avg GF	Avg FI
Control	CS1A	9.0	-1.0	55.83	54.91	3065.62	2935.78	29.39	2386.90	28.89
	CS2A	7.5	-0.7	59.14	50.58	2991.32	2507.25	35.82		
	CS4A	5.5	-0.8	58.11	55.10	3202.00	1717.68	21.47		
BS5	BS51A	3.5	-0.6	50.43	52.19	2631.82	1329.88	22.17	1614.78	21.74
	BS53B	5.4	-1.0	62.83	51.52	3236.59	1668.42	16.68		
	BS54B	5.5	-0.7	58.82	50.65	2979.36	1846.03	26.37		
BF5	BF51A	3.5	-0.7	56.12	49.50	2777.82	1259.98	18.00	1829.67	16.09
	BF53A	4.9	-0.9	55.13	50.61	2789.60	1756.52	19.52		
	BF53B	7.0	-2.3	56.16	50.41	2831.15	2472.49	10.75		
BS10	BS101A	5.0	-0.1	63.13	51.69	3263.00	1532.33	153.23	1587.26	104.90
	BS102B	5.7	-0.2	60.10	50.69	3046.22	1871.17	93.56		
	BS103A	4.1	-0.2	59.27	50.93	3018.52	1358.28	67.91		
BF10	BF101A	6.1	-0.3	59.48	50.61	3010.56	2026.20	67.54	1973.02	75.14
	BF101B	6.7	-0.3	60.22	50.43	3036.72	2206.33	73.54		
	BF102B	5.5	-0.2	64.17	50.82	3261.15	1686.52	84.33		

Curriculum Vitae

Candidate's full name:

Oluwasewa Olanike Owolabi

Universities attended:

University of Prince Edward Island

Engineering Diploma

2017

University of New Brunswick

B.Sc. Civil Engineering

2019

Publication:

Sanchez, X., Somers, T., Dhasmana, H., Owolabi, O. (2020). *Effect of Biochar on the Basic Characteristics of Asphalt Mixtures*. Papagiannakis, A.T., Anupam, K., Bhasin, A., & Little, D. (Eds.). (2020). Advances in Materials and Pavement Performance Prediction II: Contributions to the 2nd International Conference on Advances in Materials and Pavement Performance Prediction (AM3P 2020), 27-29 May 2020, San Antonio, TX, USA (1st ed.). CRC Press. https://doi.org/10.1201/9781003027362

Conference Presentation:

Owolabi, O., Sanchez, X. (2021). *Effect of Biochar as a Filler in Asphalt Mixtures*. Submitted to Canadian Technical Asphalt Association 66th Annual Conference, Charlottetown, Prince Edward Island, November 2021